To appear in: **Mathematical Sciences**

Online ISSN: 2251-7456 Print ISSN: 2008-1359

Received: 9 December 2025
Revised: 28 December 2025
Accepted: 27 January 2026

DOI:10.57647/mathsci.2026.97471

Rotation Effects on a Nonlocal Micropolar Double-Porous Medium with Variable Conductivity and Initial Stress Using MGT Theory

Doaa. M. Salah[1], A.M. Abd-Alla[1,*], SMM El-Kabeir[2] , Kawther K. Alarfaj[3]
[1]Department of Mathematics, Faculty of Science, Sohag University, Egypt

[2]Department of Mathematics, Faculty of Science, Aswan University, Egypt
[3]Department of Mathematics and Statistics, College of Science, King Faisal University, Al-Ahsa, P.O. Box 400, Saudi Arabia

[*]Corresponding Author: mohmrr@yahoo.com

Doaa. M. Salah https://orcid.org/0000-0001-9220-1413

Abdelmooty Abdalla https://orcid.org/0000-0002-6839-3731

Saber El-Kabeir https://orcid.org/0000-0002-9468-9368

Kawther K. Alarfaj https://orcid.org/0009-0007-8530-1329

Abstract:

This study investigates the two-dimensional behavior of a nonlocal micropolar double-porous thermoelastic material with voids (MDPTMWV) within the framework of the Moore–Gibson–Thompson (MGT) theory. An isotropic, homogeneous, initially stressed, rotating thermoelastic half-space with double porosity is considered. The MGT heat conduction model, incorporating memory-dependent derivatives and variable thermal conductivity, is employed. Governing equations are derived using generalized thermoelasticity, and analytical solutions for displacement, temperature, equilibrated stress, and thermal stress components are obtained via Lame's potentials combined with normal mode analysis. The model is analyzed under boundary conditions including variable temperature, normal stress, constant equilibrated stress, and stress-free surfaces. Numerical evaluations using MATHEMATICA illustrate the effects of time, rotation, initial stress, and nonlocal parameters. The results indicate that double porosity and the considered parameters significantly amplify material responses, particularly under increasing time, rotation, initial stress, and nonlocal effects. Several special cases are discussed and validated against the literature. These findings provide insights relevant to geophysics, seismology, and earthquake engineering.

Keywords: Rotation, Initial stress, Nonlocal parameter, Micropolar double-porous medium, MGT thermoelasticity, Normal mode analysis.

Nomenclature

ρ Material density

θ Thermodynamic temperature

$\theta_\circ$ Reference temperature

u, w Displacement components

μ_{ij} Nonlocal couple stress tensor

σ_{ij} Nonlocal stress tensor

Φ, Ψ Scalar functions

c_e Specific heat

λ, μ Lame's constants

η, K Micropolar material constants

L_N Nonlocal parameter

ϖ Microinertia

ϵ Time relaxation parameter

α_t Coefficient of linear thermal expansion

k Temperature-dependent thermal conductivity

k^* Temperature-dependent material property corresponding to the rate of conductivity

k_d Thermal diffusivity

k_o Thermal conductivity at reference temperature θ_o

k_o^* Material property corresponding to the rate of conductivity at reference temperature θ_o

υ Dilatation term

β_1^*, β_2^* Void parameters

$\vartheta_1, \vartheta_2, \vartheta_3$ Void parameters

$\xi^*_1, \xi^*_2, \xi^*_3$ Void parameters

$\gamma_1, \upsilon_1, \upsilon_2$ Thermal parameters

q_1, q_2 Volume fractions of matrix and fracture pores, respectively

Π_1, Π_2 Equilibrated inertia of matrix and fracture pores, respectively

p Initial stress

$\vec{\varphi}$ Microrotation vector

ϕ Thermal displacement

Ω Rotation parameter

t Time

σ_{ij} Stress components

σ_i , ς_i Nonlocal equilibrated stress vectors of matrix and fracture pores, respectively

b Wave number

ω Angular frequency

1. Introduction

The propagation of thermoelastic waves and the associated memory effects in solid media have emerged as fundamental topics in modern continuum mechanics, owing to their critical relevance in geophysical processes, biomedical applications, aerospace structures, and advanced functional materials. Accurately describing such phenomena requires sophisticated theoretical models capable of capturing microstructural interactions, porosity, thermal relaxation, and nonlocal effects. These features become particularly significant under rapid thermal loading, high-frequency excitations, and small-scale configurations, where classical thermoelastic formulations are no longer adequate. At micro- and nano-length scales, nonlocal elasticity provides a more realistic representation of material behavior by incorporating long-range interactions between material points, thereby overcoming the inherent limitations of local continuum theories. This approach is especially important for materials with pronounced microstructural heterogeneity. In parallel, the consideration of variable thermal conductivity allows for a more faithful description of heat transfer in functionally graded materials and thermally adaptive composites, where thermal properties may vary spatially or depend on temperature. The coupled thermo-mechanical response arising from these effects plays a pivotal role in determining the overall dynamic behavior of thermoelastic bodies. A variety of thermoelastic theories have been proposed to investigate the coupling between thermal and mechanical fields, and numerous studies [1–5] have explored the interaction between temperature, displacement, and related physical variables. Further advancements in this area include investigations of wave propagation and initial stress effects in complex thermoelastic media. In this regard, Boora et al. [6] analyzed wave

reflection in a thermodiffusion medium with double porosity, while Othman et al. [7] examined the influence of initial stress in thermoelastic media containing voids and micro temperatures. Nonlocal thermoelasticity, commonly formulated within the framework of Eringen's nonlocal elasticity theory [8], extends classical thermoelastic models by incorporating spatial interactions over finite distances. This formulation has proven particularly effective in modeling nanobeams, nanoplates, and other micro- and nano-scale structures, where classical theories are unable to predict experimentally observed size-dependent responses. Consequently, nonlocal thermoelastic models have become indispensable in the analysis and design of MEMS and NEMS devices. Several investigators [9–12] have examined the thermo-mechanical behavior of thermoelastic media using different generalized theories while accounting for various physical parameters and loading conditions. Among advanced thermoelastic frameworks, the Moore–Gibson–Thompson (MGT) theory represents a substantial advancement in the modeling of heat conduction and thermoelastic wave propagation. Unlike the classical Fourier law, which implies an unphysical infinite speed of thermal signal propagation, the MGT theory introduces a third-order time derivative in the heat conduction equation, thereby incorporating finite thermal wave speeds and intrinsic memory effects. This formulation yields a hyperbolic heat conduction model that ensures thermodynamic consistency and provides a more realistic description of wave attenuation and energy dissipation, particularly in transient and high-frequency thermal processes. The effectiveness of the MGT theory has been demonstrated across a broad spectrum of applications, including laser–material interactions, thermoacoustic devices, high-intensity focused ultrasound, and thermal stress analysis in micro- and nano-electromechanical systems. Recent research has further extended the MGT framework to increasingly complex material models. Gupta et al. [13] investigated memory-dependent thermoelastic responses in a nonlocal micropolar double-porous medium under the MGT theory, while Awwad et al. [14] analyzed thermoelastic behavior in media with temperature-dependent properties. Additional contributions by Gupta et al. [15] and Kumar et al. [16] explored fractional-order and photo-thermoelastic models within the MGT framework. Moreover, Tiwari et al. [17] incorporated nonlocal effects into a generalized thermoelastic medium with memory, whereas Kumar and Vohra [18] studied pulsed laser heating in a thermoelastic microbeam with double porosity. Abouelregal et al. [19] applied the MGT model to investigate laser-induced thermoelastic responses in a microbeam resting on a viscoelastic foundation, and Alhassan et al. [20] proposed a modified fractional MGT

formulation to capture anomalous thermal diffusion in elastic media with cylindrical cavities. Similar analytical and numerical techniques have been applied to thermoelastic media with microstructural effects, nonlocal interactions, and memory-dependent heat conduction [21–23]. Moreover, advanced mathematical approaches have been widely used to analyze coupled thermal and mechanical transport phenomena in complex continua, providing a broader methodological background for the present work [24–29]. Recent studies have examined the effects of nonlocality, rotation, diffusion, and double porosity on thermoelastic media, demonstrating their significant influence on wave propagation and stress distribution [30, 31]. However, the combined influence of nonlocality, micropolar effects, double porosity, variable thermal conductivity, rotation, and initial stress within the Moore–Gibson–Thompson thermoelastic framework has not yet been comprehensively addressed.

Motivated by this gap, the present study develops a unified theoretical model to analyze the memory-dependent thermoelastic behavior of a rotating nonlocal micropolar double-porous medium under the MGT theory. The governing equations are formulated within the context of generalized thermoelasticity, and analytical solutions for displacement, temperature, equilibrated stress, shear stress, and normal stress are derived using Lame's potentials in conjunction with the normal mode method. A detailed parametric investigation is carried out to examine the effects of initial stress, rotation, time, and nonlocal parameters, with numerical results presented graphically to elucidate their significant influence on thermoelastic wave propagation and stress distribution.

2. Formulation of the problem

The problem is formulated in the two-dimensional $x - z$ plane with the z-axis directed downward. A semi-infinite, homogeneous, isotropic, rotating nonlocal micropolar double-porous thermoelastic medium with variable thermal conductivity (MDPTMWV) is considered, governed by the memory-dependent Moore–Gibson–Thompson (MGT) theory. The medium is subjected to uniform initial stress and initially maintained at a reference temperature θ_0. Due to the two-dimensional deformation, the displacement and microrotation vectors are taken as $\vec{u} = (u, 0, w)$, $\vec{\varphi} = (0, \varphi_2, 0)$. Thermal conductivity and specific heat vary linearly with temperature, introducing nonlinearity into the MGT heat conduction equation, with $k = k_o\ (1 + k_1\theta)$, $k^* = k^*_o\ (1 + k_2\ \phi)$, and thermal diffusivity ($k_d = \frac{k}{\rho c_e}$) assumed constant. The governing equations arise from the balance laws of linear and angular momentum under rotation and initial stress, coupled with the MGT heat conduction law,

yielding a system of partial differential equations for displacement, microrotation, porosity, and temperature fields. The equations, expressed in Cartesian coordinates, are presented below [13].

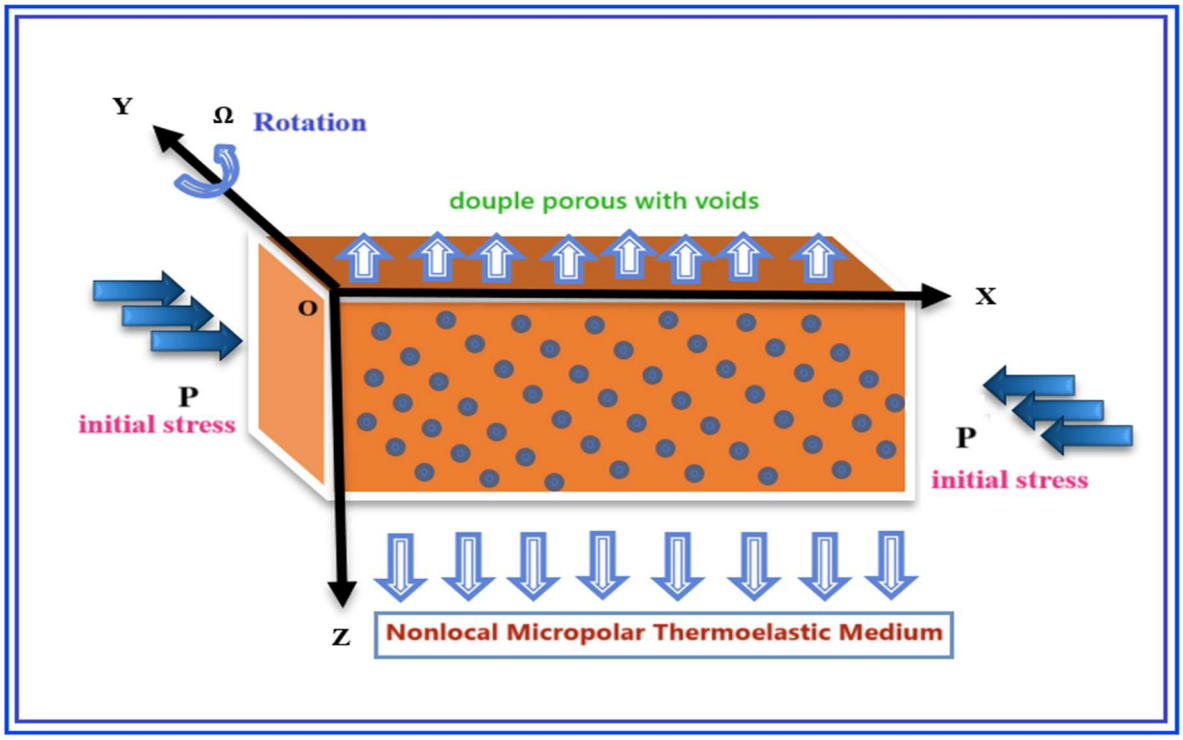

Figure 1: Problem Geometry.

The equations of motion are [13]

$$\rho\left(1-L_N{}^2\nabla^2\right)\frac{\partial^2 u}{\partial t^2}-\rho\Omega^2 u+2\rho\Omega\frac{\partial w}{\partial t}=\left(\lambda+2\mu+\frac{p}{2}+K\right)\frac{\partial^2 u}{\partial x^2}+\left(\lambda+\mu+\frac{p}{2}\right)\frac{\partial^2 w}{\partial x\partial z}+$$
$$\left(\mu-\frac{p}{2}+K\right)\frac{\partial^2 u}{\partial z^2}-K\frac{\partial\varphi_2}{\partial z}-\gamma_1\frac{\partial}{\partial x}\left(\frac{-1+\sqrt{1+2k_1T_1}}{k_1}\right)+\beta_1^*\frac{\partial q_1}{\partial x}+\beta_2^*\frac{\partial q_2}{\partial x}, \quad (1)$$

$$\rho\left(1-L_N{}^2\nabla^2\right)\frac{\partial^2 w}{\partial t^2}-\rho\Omega^2 w-2\rho\Omega\frac{\partial u}{\partial t}=\left(\lambda+2\mu+\frac{p}{2}+K\right)\frac{\partial^2 w}{\partial z^2}+\left(\lambda+\mu+\frac{p}{2}\right)\frac{\partial^2 u}{\partial x\partial z}+$$
$$\left(\mu-\frac{p}{2}+K\right)\frac{\partial^2 w}{\partial x^2}+K\frac{\partial\varphi_2}{\partial x}-\gamma_1\frac{\partial}{\partial z}\left(\frac{-1+\sqrt{1+2k_1T_1}}{k_1}\right)+\beta_1^*\frac{\partial q_1}{\partial z}+\beta_2^*\frac{\partial q_2}{\partial z}, \quad (2)$$

The heat conduction for thermoelasticity with memory dependent derivative is [13]

$$\frac{\partial}{\partial t}\left[\frac{\partial^2 T_1}{\partial x^2}+\frac{\partial^2 T_1}{\partial z^2}\right]+\frac{k_o{}^*}{k_o}\left[\frac{\partial^2 T_1}{\partial x^2}+\frac{\partial^2 T_1}{\partial z^2}\right]=(1+\epsilon D_\epsilon)\left[\frac{1}{k_d}\frac{\partial^2 T_1}{\partial t^2}+\frac{\theta_o}{k_o}\frac{\partial^2}{\partial t^2}(\gamma_1 v+v_1 q_1+v_2 q_2)\right], \quad (3)$$

The nonlocal couple stress equation of motion is

$$\left(1-L_N{}^2\nabla^2\right)\rho\varpi\frac{\partial^2\varphi_2}{\partial t^2}=\eta\nabla^2\varphi_2+K\left(\frac{\partial u}{\partial z}-\frac{\partial w}{\partial x}\right)-2K\varphi_2, \quad (4)$$

The equilibrated stress equations of motions due to voids and nonlocal are [13]

$$-\beta_1^*\left(\frac{\partial u}{\partial x}+\frac{\partial w}{\partial z}\right)+\vartheta_1\left(\frac{\partial^2 q_1}{\partial x^2}+\frac{\partial^2 q_1}{\partial z^2}\right)+\vartheta_2\left(\frac{\partial^2 q_2}{\partial x^2}+\frac{\partial^2 q_2}{\partial z^2}\right)-\xi^*{}_1 q_1-\xi^*{}_2 q_2+v_1\left(\frac{-1+\sqrt{1+2k_1T_1}}{k_1}\right)$$

$$=\Pi_1\left(1-{L_N}^2\nabla^2\right)\frac{\partial^2 q_1}{\partial t^2}, \tag{5}$$

$$-\beta_2^*\left(\frac{\partial u}{\partial x}+\frac{\partial w}{\partial z}\right)+\vartheta_2\left(\frac{\partial^2 q_1}{\partial x^2}+\frac{\partial^2 q_1}{\partial z^2}\right)+\vartheta_3\left(\frac{\partial^2 q_2}{\partial x^2}+\frac{\partial^2 q_2}{\partial z^2}\right)-\xi^*{}_2 q_1-\xi^*{}_3 q_2+v_2\left(\frac{-1+\sqrt{1+2k_1T_1}}{k_1}\right)$$

$$=\Pi_2\left(1-{L_N}^2\nabla^2\right)\frac{\partial^2 q_1}{\partial t^2}, \tag{6}$$

The stress components are

$$\sigma_{xx}=-p+(\lambda+2\mu+K)\frac{\partial u}{\partial x}+\lambda\frac{\partial w}{\partial z}+\beta_1^* q_1\ +\beta_2^* q_2-\gamma_1\left(\frac{-1+\sqrt{1+2k_1T_1}}{k_1}\right), \tag{7}$$

$$\sigma_{zz}=-p+\lambda\frac{\partial u}{\partial x}+(\lambda+2\mu+K)\frac{\partial w}{\partial z}+\beta_1^* q_1\ +\beta_2^* q_2-\gamma_1\left(\frac{-1+\sqrt{1+2k_1T_1}}{k_1}\right), \tag{8}$$

$$\sigma_{xz}=\left(\mu+\frac{p}{2}+K\right)\frac{\partial u}{\partial z}+\left(\mu-\frac{p}{2}\right)\frac{\partial w}{\partial x}-K\varphi_2, \tag{9}$$

The equilibrated stress corresponding to voids

$$\sigma_x=\vartheta_1\frac{\partial q_1}{\partial x}+\vartheta_2\frac{\partial q_2}{\partial x}, \tag{10}$$

$$\sigma_z=\vartheta_1\frac{\partial q_1}{\partial z}+\vartheta_2\frac{\partial q_2}{\partial z}, \tag{11}$$

$$\varsigma_x=\vartheta_2\frac{\partial q_1}{\partial x}+\vartheta_3\frac{\partial q_2}{\partial x}, \tag{12}$$

$$\varsigma_z=\vartheta_2\frac{\partial q_1}{\partial z}+\vartheta_3\frac{\partial q_2}{\partial z}, \tag{13}$$

The local couple stress

$$\mu_{zy}=\eta\frac{\partial \varphi_2}{\partial z}, \tag{14}$$

$$\mu_{xy}=\eta\frac{\partial \varphi_2}{\partial x}, \tag{15}$$

The local equilibrated body forces

$$\Xi_1=-\beta_1^*\left(\frac{\partial u}{\partial x}+\frac{\partial w}{\partial z}\right)-\xi^*{}_1 q_1-\xi^*{}_2 q_2+v_1\left(\frac{-1+\sqrt{1+2k_1T_1}}{k_1}\right), \tag{16}$$

$$\Xi_2=-\beta_2^*\left(\frac{\partial u}{\partial x}+\frac{\partial w}{\partial z}\right)-\xi^*{}_2 q_1-\xi^*{}_3 q_2+v_2\left(\frac{-1+\sqrt{1+2k_1T_1}}{k_1}\right). \tag{17}$$

To felicitate numerical computations, the following quantities are defined which are dimensionless,

$$(\acute{x},\acute{z}) = \frac{c_1}{k_d}\,(x,z), (\acute{u},\acute{w}) = \frac{c_1}{k_d}\,(u,w), (\acute{q_1},\acute{q_2}) = \frac{\Pi_1 c_1^4}{\beta_1^* {k_d}^2}\,(q_1,q_2),\ \theta' = \frac{\theta}{\theta_o},\ \acute{\Omega} = \frac{k_d}{c_1^2}\Omega,$$

$$\sigma'_{ij} = \frac{\sigma_{ij}}{\lambda+2\mu+p+K},\ \sigma'_i = \frac{k_d}{c_1}\sigma_i,\ (t',\epsilon') = \frac{c_1^2}{k_d}(t,\epsilon), \left(\acute{T_1},\acute{T_2}\right) = \frac{1}{\theta_o}(T_1,T_2),\ \acute{\varphi}_2 = \varphi_2,$$

$$\mu'_{ij} = \frac{c_1}{\gamma_1\theta_o k_d}\mu_{ij},\ (\sigma'_i,\varsigma'_i) = \frac{k_d}{\vartheta_1 c_1}(\sigma_i,\varsigma_i),\ c_1^2 = \frac{\lambda+2\mu+K}{\rho}. \tag{18}$$

Using (18) in (1)-(17) after removing the primes, we obtain

$$\left(1 - a_o {L_N}^2\nabla^2\right)\frac{\partial^2 u}{\partial t^2} - \Omega^2 u + 2\Omega\frac{\partial w}{\partial t} = r_1\frac{\partial^2 u}{\partial x^2} + r_2\frac{\partial^2 w}{\partial x\partial z} + r_3\frac{\partial^2 u}{\partial z^2} - r_4\frac{\partial \varphi_2}{\partial z} - r_5\frac{\partial T_1}{\partial x} + r_6\frac{\partial q_1}{\partial x} + r_7\frac{\partial q_2}{\partial x}, \tag{19}$$

$$\left(1 - a_o {L_N}^2\nabla^2\right)\frac{\partial^2 w}{\partial t^2} - \Omega^2 w + 2\Omega\frac{\partial u}{\partial t} = r_1\frac{\partial^2 w}{\partial z^2} + r_2\frac{\partial^2 u}{\partial x\partial z} + r_3\frac{\partial^2 w}{\partial x^2} + r_4\frac{\partial \varphi_2}{\partial x} - r_5\frac{\partial T_1}{\partial z} + r_6\frac{\partial q_1}{\partial z} + r_7\frac{\partial q_2}{\partial z}, \tag{20}$$

$$\frac{\partial}{\partial t}\left[\frac{\partial^2 T_1}{\partial x^2} + \frac{\partial^2 T_1}{\partial z^2}\right] + r_8\left[\frac{\partial^2 T_1}{\partial x^2} + \frac{\partial^2 T_1}{\partial z^2}\right] = (1 + a_1\epsilon D_\epsilon)\left[\frac{\partial^2 T_1}{\partial t^2} + r_9\frac{\partial^2}{\partial t^2}\left(\frac{\partial u}{\partial x} + \frac{\partial w}{\partial z}\right) + r_{10}\frac{\partial^2 q_1}{\partial t^2} + r_{11}\frac{\partial^2 q_2}{\partial t^2}\right], \tag{21}$$

$$\left(1 - a_o {L_N}^2\nabla^2\right)\frac{\partial^2 \varphi_2}{\partial t^2} = r_{12}\nabla^2\varphi_2 + r_{13}\left(\frac{\partial u}{\partial z} - \frac{\partial w}{\partial x}\right) - r_{14}\varphi_2, \tag{22}$$

$$-\left(\frac{\partial u}{\partial x} + \frac{\partial w}{\partial z}\right) + r_{15}\left(\frac{\partial^2 q_1}{\partial x^2} + \frac{\partial^2 q_1}{\partial z^2}\right) + r_{16}\left(\frac{\partial^2 q_2}{\partial x^2} + \frac{\partial^2 q_2}{\partial z^2}\right) - r_{17}q_1 - r_{18}q_2 + r_{19}T_1$$

$$= \left(1 - a_o {L_N}^2\nabla^2\right)\frac{\partial^2 q_1}{\partial t^2}, \tag{23}$$

$$-r_{20}\left(\frac{\partial u}{\partial x} + \frac{\partial w}{\partial z}\right) + r_{21}\left(\frac{\partial^2 q_1}{\partial x^2} + \frac{\partial^2 q_1}{\partial z^2}\right) + r_{22}\left(\frac{\partial^2 q_2}{\partial x^2} + \frac{\partial^2 q_2}{\partial z^2}\right) - r_{23}q_1 - r_{24}q_2 + r_{25}T_1$$

$$= \left(1 - a_o {L_N}^2\nabla^2\right)\frac{\partial^2 q_1}{\partial t^2}, \tag{24}$$

$$\sigma_{xx} = s_o + \frac{\partial u}{\partial x} + r_o\frac{\partial w}{\partial z} - r_5 T_1 + r_6 q_1 + r_7 q_2, \tag{25}$$

$$\sigma_{zz} = s_o + r_o\frac{\partial u}{\partial x} + \frac{\partial w}{\partial z} - r_5 T_1 + r_6 q_1 + r_7 q_2\ , \tag{26}$$

$$\sigma_{xz} = n_1\frac{\partial u}{\partial z} + n_2\frac{\partial w}{\partial x} - r_4\varphi_2, \tag{27}$$

$$\sigma_x = n_3\frac{\partial q_1}{\partial x} + n_4\frac{\partial q_2}{\partial x}, \tag{28}$$

$$\sigma_z = n_3\frac{\partial q_1}{\partial z} + n_4\frac{\partial q_2}{\partial z}, \tag{29}$$

$$\varsigma_x = n_4 \frac{\partial q_1}{\partial x} + n_5 \frac{\partial q_2}{\partial x}, \tag{30}$$

$$\varsigma_z = n_4 \frac{\partial q_1}{\partial z} + n_5 \frac{\partial q_2}{\partial z}, \tag{31}$$

$$\mu_{zy} = n_6 \frac{\partial \varphi_2}{\partial z}, \tag{32}$$

$$\mu_{xy} = n_6 \frac{\partial \varphi_2}{\partial x}. \tag{33}$$

where

$$a_o = \frac{c_1^2}{k_d^2}, a_1 = \frac{k_d}{c_1^2}, r_o = \frac{\lambda}{\lambda+2\mu+K}, \; r_1 = \frac{(\lambda+2\mu+\frac{p}{2}+K)k_d}{\lambda+2\mu+K}, r_2 = \frac{\lambda+\mu+\frac{p}{2}}{\lambda+2\mu+K}, r_3 = \frac{\mu-\frac{p}{2}+K}{\lambda+2\mu+K},$$

$$r_4 = \frac{K}{\lambda+2\mu+K}, r_5 = \frac{\gamma_{1\theta_o}}{\lambda+2\mu+K}, r_6 = \frac{\beta_1^{*2}{k_d}^2}{\Pi_1 c_1^4(\lambda+2\mu+K)}, r_7 = \frac{\beta_1^*\beta_2^*{k_d}^2}{\Pi_1 c_1^4(\lambda+2\mu+K)}, \; r_8 = \frac{{k_o}^* k_d}{k_o c_1^2},$$

$$r_9 = \frac{\gamma_1 k_d}{k_o}, r_{10} = \frac{v_1\beta_1^*{k_d}^3}{k_o\,\Pi_1 c_1^4}, r_{11} = \frac{v_2\beta_1^*{k_d}^3}{k_o\,\Pi_1 c_1^4}, r_{12} = \frac{\eta}{\rho\varpi\ _1^2}, r_{13} = \frac{K{k_d}^2}{\rho\varpi c_1^4}, r_{14} = \frac{2K{k_d}^2}{\rho\varpi\ _1^4},$$

$$r_{15} = \frac{\vartheta_1}{\Pi_1 c_1^2}, r_{16} = \frac{\vartheta_2}{\Pi_1 c_1^2}, r_{17} = \frac{\xi^*{}_1{k_d}^2}{\Pi_1 c_1^4}, r_{18} = \frac{\xi^*{}_2{k_d}^2}{\Pi_1 c_1^4}, r_{19} = \frac{v_1\theta_o}{\beta_1^*}, r_{20} = \frac{\beta_2^*\Pi_1}{\beta_1^*\Pi_2},$$

$$r_{21} = \frac{\vartheta_2}{\Pi_2 c_1^2}, r_{22} = \frac{\vartheta_3}{\Pi_2 c_1^2}, r_{23} = \frac{\xi^*{}_2{k_d}^2}{\Pi_2 c_1^4}, r_{24} = \frac{\xi^*{}_3{k_d}^2}{\Pi_2 c_1^4}, r_{25} = \frac{v_2\Pi_1\theta_o}{\Pi_2\,\beta_1^*}, S_o = \frac{-p}{\lambda+2\mu+K},$$

$$n_1 = \frac{\mu+\frac{p}{2}+K}{\lambda+2\mu+K}, n_2 = \frac{\mu-\frac{p}{2}}{\lambda+2\mu+K}, n_3 = \frac{\beta_1^*{k_d}^2}{\Pi_1 c_1^4}, n_4 = \frac{\vartheta_2\beta_1^*{k_d}^2}{\vartheta_1\,\Pi_1 c_1^4}, n_5 = \frac{\vartheta_3\beta_1^*{k_d}^2}{\vartheta_1\,\Pi_1 c_1^4}, n_6 = \frac{\eta c_1^2}{\gamma_{1\theta_o} k_d^2}.$$

3. Solution of the problem

Using Helmholtz's representation, the displacement components may be expressed in terms of scalar and vector potential functions,

$$u = \frac{\partial \Phi}{\partial x} - \frac{\partial \Psi}{\partial z}, w = \frac{\partial \Phi}{\partial z} + \frac{\partial \Psi}{\partial x}. \tag{34}$$

Using the representation (34) in (19)-(24), we obtain the equations in decoupled form

$$\left(1 - a_o {L_N}^2 \nabla^2\right)\frac{\partial^2 \Phi}{\partial t^2} - \Omega^2 \Phi = r_1 \frac{\partial^2 \Phi}{\partial x^2} + r_{26}\frac{\partial^2 \Phi}{\partial z^2} - r_5 T_1 + r_6 q_1 + r_7 q_2, \tag{35}$$

$$\left(1 - a_o {L_N}^2 \nabla^2\right)\frac{\partial^2 \Psi}{\partial t^2} - \Omega^2 \Psi = r_3 \frac{\partial^2 \Psi}{\partial x^2} + r_{27}\frac{\partial^2 \Psi}{\partial z^2} + r_4 \varphi_2, \tag{36}$$

$$\frac{\partial}{\partial t}\left[\frac{\partial^2 T_1}{\partial x^2} + \frac{\partial^2 T_1}{\partial z^2}\right] + r_8\left[\frac{\partial^2 T_1}{\partial x^2} + \frac{\partial^2 T_1}{\partial z^2}\right] =$$

$$(1 + a_1 \epsilon D_\epsilon)\left[\frac{\partial^2 T_1}{\partial t^2} + r_9 \frac{\partial^2}{\partial t^2}\left(\frac{\partial^2 \Phi}{\partial x^2} + \frac{\partial^2 \Phi}{\partial z^2}\right) + r_{10}\frac{\partial^2 q_1}{\partial t^2} + r_{11}\frac{\partial^2 q_2}{\partial t^2}\right], \tag{37}$$

$$\left(1 - a_o {L_N}^2 \nabla^2\right) \frac{\partial^2 \varphi_2}{\partial t^2} = r_{12} \nabla^2 \varphi_2 - r_{13} \left(\frac{\partial^2 \Psi}{\partial x^2} + \frac{\partial^2 \Psi}{\partial z^2}\right) - r_{14} \varphi_2, \tag{38}$$

$$-\left(\frac{\partial^2 \Phi}{\partial x^2} + \frac{\partial^2 \Phi}{\partial z^2}\right) + r_{15} \left(\frac{\partial^2 q_1}{\partial x^2} + \frac{\partial^2 q_1}{\partial z^2}\right) + r_{16} \left(\frac{\partial^2 q_2}{\partial x^2} + \frac{\partial^2 q_2}{\partial z^2}\right) - r_{17} q_1 - r_{18} q_2 + r_{19} T_1$$

$$= \left(1 - a_o {L_N}^2 \nabla^2\right) \frac{\partial^2 q_1}{\partial t^2}, \tag{39}$$

$$-r_{20} \left(\frac{\partial^2 \Phi}{\partial x^2} + \frac{\partial^2 \Phi}{\partial z^2}\right) + r_{21} \left(\frac{\partial^2 q_1}{\partial x^2} + \frac{\partial^2 q_1}{\partial z^2}\right) + r_{22} \left(\frac{\partial^2 q_2}{\partial x^2} + \frac{\partial^2 q_2}{\partial z^2}\right) - r_{23} q_1 - r_{24} q_2 + r_{25} T_1$$

$$= \left(1 - a_o {L_N}^2 \nabla^2\right) \frac{\partial^2 q_1}{\partial t^2}, \tag{40}$$

$$\sigma_{xx} = s_o + \frac{\partial^2 \Phi}{\partial x^2} + r_o \frac{\partial^2 \Phi}{\partial z^2} + (r_o - 1) \frac{\partial^2 \Psi}{\partial x \partial z} - r_5 T_1 + r_6 q_1 + r_7 q_2, \tag{41}$$

$$\sigma_{zz} = s_o + r_o \frac{\partial^2 \Phi}{\partial x^2} + \frac{\partial^2 \Phi}{\partial z^2} + (1 - r_o) \frac{\partial^2 \Psi}{\partial x \partial z} - r_5 T_1 + r_6 q_1 + r_7 q_2, \tag{42}$$

$$\sigma_{xz} = (n_1 + n_2) \frac{\partial^2 \Phi}{\partial x \partial z} + n_2 \frac{\partial^2 \Psi}{\partial x^2} - n_1 \frac{\partial^2 \Psi}{\partial z^2} - r_4 \varphi_2, \tag{43}$$

$$\sigma_x = n_3 \frac{\partial q_1}{\partial x} + n_4 \frac{\partial q_2}{\partial x}, \tag{44}$$

$$\sigma_z = n_3 \frac{\partial q_1}{\partial z} + n_4 \frac{\partial q_2}{\partial z}, \tag{45}$$

$$\varsigma_x = n_4 \frac{\partial q_1}{\partial x} + n_5 \frac{\partial q_2}{\partial x}, \tag{46}$$

$$\varsigma_z = n_4 \frac{\partial q_1}{\partial z} + n_5 \frac{\partial q_2}{\partial z}, \tag{47}$$

$$\mu_{zy} = n_6 \frac{\partial \varphi_2}{\partial z}, \tag{48}$$

$$\mu_{xy} = n_6 \frac{\partial \varphi_2}{\partial x}. \tag{49}$$

The decoupled equations obtained in the previous section are solved by assuming the solution in the form of modes:

$$\left(\Phi, \Psi, q_1, q_2, u\ , w, T_1, \varphi_2, \sigma_{ij}, \sigma_i, \mu_{ij}, \varsigma_i\right)(x, z, t) =$$

$$\left(\Phi^*, \Psi^*, {q_1}^*, {q_2}^*, u^*, w^*, {T_1}^*, {\varphi_2}^*, {\sigma_{ij}}^*, {\sigma_i}^*, {\mu_{ij}}^*, {\varsigma_i}^*\right)(x) e^{(\omega t + i\ \ )}. \tag{50}$$

This transformation expresses the field variables in terms of separable harmonic modes, thereby simplifying the system and facilitating a deeper understanding of the dynamic response and wave characteristics of the medium. In these expressions, ω represents the angular frequency, *i* is the imaginary unit, and *b* denotes the wave number in the z-direction. By substituting equation (50), equations (35-49) transform as follows:

$$r_5 {T_1}^* + (r_{28} - r_{29}D^2)\Phi^* - r_6 {q_1}^* - r_7 {q_2}^* = 0, \quad (51)$$

$$(r_{30} - r_{31}D^2)\Psi^* - r_4 {\varphi_2}^* = 0, \quad (52)$$

$$(r_{32} - r_{33}D^2){T_1}^* + (r_{34}D^2 - r_{35})\Phi^* + r_{36}{q_1}^* + r_{37}{q_2}^* = 0, \quad (53)$$

$$(r_{13}D^2 - r_{40})\Psi^* + (r_{38} - r_{39}D^2){\varphi_2}^* = 0, \quad (54)$$

$$r_{19}{T_1}^* + (b^2 - D^2)\Phi^* + (r_{41}D^2 - r_{42}){q_1}^* + (r_{16}D^2 - r_{43}){q_2}^* = 0, \quad (55)$$

$$r_{25}{T_1}^* + (r_{44} - r_{20}D^2)\Phi^* + (r_{21}D^2 - r_{45}){q_1}^* + (r_{46}D^2 - r_{47}){q_2}^* = 0, \quad (56)$$

$${\sigma_{xx}}^* = s_o e^{-(\omega t + ibz)} + (D^2 - r_o b^2)\Phi^* + ib(r_o - 1)D\Psi^* - r_5 {T_1}^* + r_6 {q_1}^* + r_7 {q_2}^*, \quad (57)$$

$${\sigma_{zz}}^* = s_o e^{-(\omega t + ibz)} + (r_o D^2 - b^2)\Phi^* + ib(1 - r_o)D\Psi^* - r_5 {T_1}^* + r_6 {q_1}^* + r_7 {q_2}^*, \quad (58)$$

$${\sigma_{xz}}^* = ib(n_1 + n_2)D\Phi^* + (n_2 D^2 + n_1 b^2)\Psi^* - r_4 {\varphi_2}^*, \quad (59)$$

$${\sigma_x}^* = n_3 D{q_1}^* + n_4 D{q_2}^*, \quad (60)$$

$${\sigma_z}^* = ibn_3 {q_1}^* + ibn_4 {q_2}^*, \quad (61)$$

$${\varsigma_x}^* = n_4 D{q_1}^* + n_5 D{q_2}^*, \quad (62)$$

$${\varsigma_z}^* = ibn_4 {q_1}^* + ibn_5 {q_2}^*, \quad (63)$$

$${\mu_{zy}}^* = ibn_6 {\varphi_2}^*, \quad (64)$$

$${\mu_{xy}}^* = n_6 D{\varphi_2}^*. \quad (65)$$

where

$D^2 = \frac{d^2}{dx^2}$, $r_{26} = r_2 + r_3$, $r_{27} = r_1 + r_2$, $r_{28} = \omega^2 - \Omega^2 + r_{26}b^2 + a_o b^2 \omega^2 {L_N}^2$,

$r_{29} = r_1 + a_o \omega^2 {L_N}^2$, $r_{30} = \omega^2 - \Omega^2 + r_{27}b^2 + a_o b^2 \omega^2 {L_N}^2$, $r_{31} = r_3 + a_o \omega^2 {L_N}^2$,

$r_{32} = \omega b^2 + r_8 b^2 + (1 + a_1 \epsilon D_\epsilon)\omega^2$, $r_{33} = \omega + r_8$, $r_{34} = \omega^2 r_9$, $r_{35} = \omega^2 r_9 b^2$,

$r_{36} = \omega^2 r_{10}$, $r_{37} = \omega^2 r_{11}$, $r_{38} = \omega^2 - r_{12}b^2 + a_o b^2 \omega^2 {L_N}^2 + r_{14}$, $r_{39} = a_o \omega^2 {L_N}^2 + r_{12}$,

$r_{40} = r_{13}b^2$, $r_{41} = a_o \omega^2 {L_N}^2 + r_{15}$, $r_{42} = \omega^2 + r_{15}b^2 + a_o b^2 \omega^2 {L_N}^2 + r_{17}$, $r_{43} = r_{16}b^2 + r_{18}$,

$r_{44} = r_{20}b^2$, $r_{45} = r_{21}b^2 + r_{23}$, $r_{46} = a_o \omega^2 {L_N}^2 + r_{22}$, $r_{47} = \omega^2 + r_{22}b^2 + a_o b^2 \omega^2 {L_N}^2 + r_{24}$.

Eliminating $\Phi^*(x)$, ${T_1}^*(x)$, ${q_1}^*(x)$, and ${q_2}^*(x)$ from equations (51), (53), (55), and (56) yields the following eighth order.

$$[D^8 + A_{11}D^6 + A_{22}D^4 + A_{33}D^2 + A_{44}]\{\Phi^*(x),{T_1}^*(x), {q_1}^*(x),{q_2}^*(x)\} = 0. \quad (66)$$

The characteristic equation corresponding to equation (66) is:

$$\lambda^8 + A_{11}\lambda^6 + A_{22}\lambda^4 + A_{33}\lambda^2 + A_{44} = 0. \quad (67)$$

Eliminating $\Psi^*(x)$, and ${\varphi_2}^*(x)$ from equations (52), and (54) yields the following fourth order.

$$[D^4 + B_{11}D^2 + B_{22}]\{\Psi^*(x),{\varphi_2}^*(x)\} = 0. \quad (68)$$

The characteristic equation corresponding to equation (68) is:

$$\lambda^4 + B_{11}\lambda^2 + B_{22} = 0. \quad (69)$$

The definitions for the coefficients A_{11}, A_{22}, A_{33}, A_{44}, B_{11} and B_{22} involved are detailed in Appendix A.

The general solutions to equations (51)– (65), subject to the condition as x→∞, are expressed as follows:

$${T_1}^*(x) = \sum_{i=1}^{4} H_i e^{-\lambda_i x}, \quad (70)$$

$$\Phi^*(x) = \sum_{i=1}^{4} G_{1i} H_i e^{-\lambda_i x}, \quad (71)$$

$${q_1}^*(x) = \sum_{i=1}^{4} G_{2i} H_i e^{-\lambda_i x}, \quad (72)$$

$${q_2}^*(x) = \sum_{i=1}^{4} G_{3i} H_i e^{-\lambda_i x}, \quad (73)$$

$$\Psi^*(x) = \sum_{j=1}^{2} H_{1j} e^{-\lambda_{1j} x}, \quad (74)$$

$${\varphi_2}^*(x) = \sum_{j=1}^{2} G_{4j} H_{1j} e^{-\lambda_{1j} x}. \quad (75)$$

The displacement components can be calculated as follows using equations (34), (71) and (74):

$$\mathrm{u}^*(x) = \sum_{i=1}^{4} -\lambda_i G_{1i} H_i e^{-\lambda_i x} + \sum_{j=1}^{2} \lambda_{1j} H_{1j} e^{-\lambda_{1j} x}, \quad (76)$$

$$\mathrm{w}^*(x) = \sum_{i=1}^{4} ibG_{1i} H_i e^{-\lambda_i x} - \sum_{j=1}^{2} \lambda_{1j} H_{1j} e^{-\lambda_{1j} x}. \quad (77)$$

where $\lambda_{i,i=1:4}$ and λ_{1j}, $j = 1{:}\,2$ are the all roots for the equation (67) and (69).

By using equations (57-65), and (34), the stress components can be determined as follows:

$$\sigma_{xx}{}^{*} = s_o e^{-(\omega t + ibz)} - \sum_{i=1}^{4} G_{5i} H_i e^{-\lambda_i x} - \sum_{j=1}^{2} G_{6j} H_{1j} e^{-\lambda_{1j} x}, \quad (78)$$

$$\sigma_{zz}{}^{*} = s_o e^{-(\omega t + \quad)} - \sum_{j=1}^{2} G_{6j} H_{1j} e^{-\lambda_{1j} x} + \sum_{i=1}^{4} G_{7i} H_i e^{-\lambda_i x}, \quad (79)$$

$$\sigma_{xz}{}^{*} = \sum_{i=1}^{4} G_{8i} H_i e^{-\lambda_i x} + \sum_{j=1}^{2} G_{9j} H_{1j} e^{-\lambda_{1j} x}, \quad (80)$$

$$\sigma_{x}{}^{*} = \sum_{i=1}^{4} G_{10}\, H_i e^{-\lambda_i x}, \quad (81)$$

$$\sigma_{z}{}^{*} = \sum_{i=1}^{4} G_{11}\, H_i e^{-\lambda_i x}, \quad (82)$$

$$\varsigma_{x}{}^{*} = \sum_{i=1}^{4} G_{12}\, H_i e^{-\lambda_i x}, \quad (83)$$

$$\varsigma_{z}{}^{*} = \sum_{i=1}^{4} G_{13}\, H_i e^{-\lambda_i x}, \quad (84)$$

$$\mu_{zy}{}^{*} = \sum_{j=1}^{2} ibn_6 G_{4j} H_{1j} e^{-\lambda_{1j} x}, \quad (85)$$

$$\mu_{xy}{}^{*} = \sum_{j=1}^{2} -n_6 \lambda_{1j} G_{4j} H_{1j} e^{-\lambda_{1j} x}. \quad (86)$$

where,

$s_1 = r_5 r_{37} + r_7 r_{32}$, $s_2 = r_7 r_{33}$, $s_3 = r_{28} r_{37} - r_7 r_{35}$, $s_4 = r_{29} r_{37} - r_7 r_{34}$, $s_5 = r_6 r_{37} - r_7 r_{36}$, $s_6 = r_5 r_{16}$, $s_7 = r_7 r_{19} - r_5 r_{43}$, $s_8 = r_7 b^2 - r_{28} r_{43}$, $s_9 = r_{16} r_{28} + r_{29} r_{43} - r_7$, $s_{10} = -r_{16} r_{29}$, $s_{11} = r_6 r_{43} - r_7 r_{42}$, $s_{12} = r_7 r_{41} - r_6 r_{16}$, $s_{13} = s_1 s_{11} + s_5 s_7$, $s_{14} = s_1 s_{12} - s_2 s_{11} + s_5 s_6$, $s_{15} = s_2 s_{12}$, $s_{16} = s_3 s_{11} + s_5 s_8$, $s_{17} = s_3 s_{12} - s_4 s_{11} + s_5 s_9$, $s_{18} = s_5 s_{10} - s_4 s_{12}$,

$G_{1i} = \frac{s_{15}\lambda_i{}^4 - s_{14}\lambda_i{}^2 - s_{13}}{s_{18}\lambda_i{}^4 + s_{17}\lambda_i{}^2 + s_{16}}$, $G_{2i} = \frac{-s_6\lambda_i{}^2 - s_7 - (s_8 + s_9\lambda_i{}^2 + s_{10}\lambda_i{}^4) G_{1i}}{s_{11} + s_{12}\lambda_i{}^2}$, $G_{3i} = \frac{r_5 + (r_{28} - r_{29}\lambda_i{}^2) G_{1i} - r_6 G_{2i}}{r_7}$,

$G_{4j} = \frac{r_{30} - r_{31}\lambda_{1j}{}^2}{r_4}$, $G_{5i} = r_5 - (\lambda_i{}^2 - r_o b^2) G_{1i} - r_6 G_{2i} - r_7 G_{3i}$, $G_{6j} = ib\lambda_{1j}(r_o - 1)$,

$G_{7i} = (r_o \lambda_i{}^2 - b^2) G_{1i} - r_5 + r_6 G_{2i} + r_7 G_{3i}$, $G_{8i} = -ib\lambda_i (n_1 + n_2) G_{1i}$,

$G_{9j} = (n_2 \lambda_{1j}{}^2 + n_1 b^2) - r_4 G_{4j}$, $G_{10} = -n_3 \lambda_i G_{2i} - n_4 \lambda_i G_{3i}$, $G_{11i} = ibn_3 G_{2i} + ibn_4 G_{3i}$,

$G_{12} = -n_4 \lambda_i G_{2i} - n_5 \lambda_i G_{3i}$, $G_{13} = -ibn_4 \lambda_i G_{2i} - ibn_5 \lambda_i G_{3i}$, i=1,2,3,4, j=1,2.

4. Boundary conditions

The unknown parameters H_i and H_{1j} are evaluated by imposing specific assumptions on the boundary conditions at the free surface located at $x = 0$. These assumptions are chosen to reflect the physical nature of the problem, ensuring that the stress components vanish or satisfy appropriate continuity requirements at the boundary, which is characteristic of a traction-free surface in elastic media.

- The thermal boundary condition is described as follows

  $\theta\,(0, z, t) = L_T^*$, and $L_T^* = L_T e^{(\omega t + ibz)}$. (87)

  where L_T represents the magnitude of thermal load.
- The boundary condition for normal stress is given by:

  $\sigma_{xx}(0, z, t) = -L_M^*$, and $L_M^* = L_M e^{(\omega t + ibz)}$. (88)

  where L_M represents the magnitude of normal mechanical load.
- The boundary condition for tangential stress is defined as follows:

  $\sigma_{xz}(0, z, t) = 0.$ (89)

- The boundary condition for couple stress is defined as follows:

  $\mu_{xy}(0, z, t) = 0.$ (90)
- The boundary conditions for equilibrated stresses are defined as follows:

  $\sigma_x(0, z, t) = 0,$

  $\varsigma_x(0, z, t) = 0.$ (91)

By combining equations (87-91), a system of six equations is obtained for the constants H_1, H_2, H_3, H_4, H_{11} and H_{12}.

$$\begin{pmatrix} 1 & 1 & 1 & 1 & 0 & 0 \\ G_{51} & G_{52} & G_{53} & G_{54} & G_{61} & G_{62} \\ G_{81} & G_{82} & G_{83} & G_{84} & G_{91} & G_{92} \\ G_{101} & G_{102} & G_{103} & G_{104} & 0 & 0 \\ 0 & 0 & 0 & 0 & \lambda_{11}G_{41} & \lambda_{12}G_{42} \\ G_{121} & G_{122} & G_{123} & G_{124} & 0 & 0 \end{pmatrix} \begin{pmatrix} H_1 \\ H_2 \\ H_3 \\ H_4 \\ H_{11} \\ H_{12} \end{pmatrix} = \begin{pmatrix} R_T \\ R_M \\ 0 \\ 0 \\ 0 \\ 0 \end{pmatrix}. \quad (92)$$

where,

$\theta(x, z, t) = \frac{-1+\sqrt{1+2k_1T_1(x,z,t)}}{k_1}$, $R_T = \frac{(k_1L_T+1)^2-1}{2k_1}$, $R_M = s_o e^{-(\omega t + i\ \ )} + L_M$.

To determine the constants H_1, H_2, H_3, H_4, H_{11} and H_{12} Cramer's method is applied to Eqs.,

$$H_1 = \frac{\Delta H_1}{\Delta}, H_2 = \frac{\Delta H_2}{\Delta}, H_3 = \frac{\Delta H_3}{\Delta}, H_4 = \frac{\Delta H_4}{\Delta}, H_{11} = \frac{\Delta H_{11}}{\Delta}, H_{12} = \frac{\Delta H_{12}}{\Delta}. \quad (93)$$

The dimensionless expressions for the physical quantities (T_1, q_1, q_2, Φ, Ψ, φ_2, u, w, σ_{ij}, σ_i, ς_i, μ_{ij}) can be obtained from equations (50) through (70-86).

$$T_1(x,z,t) = \{\sum_{i=1}^{4} H_i e^{-\lambda_i x}\} e^{(\omega t + ibz)}, \quad (94)$$

$$\Phi(x,z,t) = \{\sum_{i=1}^{4} G_{1i} H_i e^{-\lambda_i x}\} e^{(\omega t + ibz)}, \quad (95)$$

$$\Psi(x,z,t) = \{\sum_{j=1}^{2} H_{1j} e^{-\lambda_{1j} x}\} e^{(\omega t + ib\ )}, \quad (96)$$

$$\varphi_2(x,z,t) = \{\sum_{j=1}^{2} G_{4j} H_{1j} e^{-\lambda_{1j} x}\} e^{(\omega t + ibz)}, \quad (97)$$

$$q_1(x,z,t) = \{\sum_{i=1}^{4} G_{2i} H_i e^{-\lambda_i x}\} e^{(\omega t + ibz)}, \quad (98)$$

$$q_2(x,z,t) = \{\sum_{i=1}^{4} G_{3i} H_i e^{-\lambda_i x}\} e^{(\omega t + ib\ )}, \quad (99)$$

$$u(x,z,t) = \{\sum_{i=1}^{4} -\lambda_i G_{1i} H_i e^{-\lambda_i x} + \sum_{j=1}^{2} \lambda_{1j} H_{1j} e^{-\lambda_{1j} x}\} e^{(\omega t + ibz)}, \quad (100)$$

$$w(x,z,t) = \{\sum_{i=1}^{4} ibG_{1i} H_i e^{-\lambda_i x} - \sum_{j=1}^{2} \lambda_{1j} H_{1j} e^{-\lambda_{1j} x}\} e^{(\omega t + i\ \ )}, \quad (101)$$

$$\sigma_{xx}(x,z,t) = \{s_o e^{-(\omega t + ibz)} - \sum_{i=1}^{4} G_{5i} H_i e^{-\lambda_i x} - \sum_{j=1}^{2} G_{6j} H_{1j} e^{-\lambda_{1j} x}\} e^{(\omega t + ibz)}, \quad (102)$$

$$\sigma_{zz}(x,z,t) = \{s_o e^{-(\omega t + i\ \ )} - \sum_{j=1}^{2} G_{6j} H_{1j} e^{-\lambda_{1j} x} + \sum_{i=1}^{4} G_{7i} H_i e^{-\lambda_i x}\} e^{(\omega t + i\ \ )}, \quad (103)$$

$$\sigma_{xz}(x,z,t) = \{\sum_{i=1}^{4} G_{8i} H_i e^{-\lambda_i x} + \sum_{j=1}^{2} G_{9j} H_{1j} e^{-\lambda_{1j} x}\} e^{(\omega t + ibz)}, \quad (104)$$

$$\sigma_x(x,z,t) = \{\sum_{i=1}^{4} G_{10i} H_i e^{-\lambda_i x}\} e^{(\omega t + i\ \ )}, \quad (105)$$

$$\sigma_z(x,z,t) = \{\sum_{i=1}^{4} G_{11}\ H_i e^{-\lambda_i x}\} e^{(\omega t + \ \ )}, \quad (106)$$

$$\varsigma_x(x,z,t) = \{\sum_{i=1}^{4} G_{12}\ H_i e^{-\lambda_i x}\} e^{(\omega t + i\ \ )}, \quad (107)$$

$$\varsigma_z(x,z,t) = \{\sum_{i=1}^{4} G_{13}\ H_i e^{-\lambda_i x}\} e^{(\omega t + i\ \ )}, \quad (108)$$

$$\mu_{zy}(x,z,t) = \{\sum_{j=1}^{2} ibn_6 G_{4j} H_{1j} e^{-\lambda_{1j} x}\} e^{(\omega t + i\ \ )}, \quad (109)$$

$$\mu_{xy}(x,z,t) = \{\sum_{j=1}^{2} -n_6 \lambda_{1j} G_{4j} H_{1j} e^{-\lambda_{1j} x}\}\ e^{(\omega t + ibz)}. \quad (110)$$

5. Numerical Results and Discussion

This section presents numerical simulations of wave propagation in a thermoelastic medium, focusing on temperature, displacement, thermal stress, and equilibrated stresses. The effects of time, rotation, initial stress, and nonlocal parameters are examined. Simulations were carried out using a Mathematica program, enabling accurate computations

and high-quality graphical visualization of spatial and temporal distributions. Magnesium crystal material properties were adopted from Gupta et al. [13] for numerical evaluation.

Unit	Symbol	Value	Unit	Symbol	Value
$\mathbf{N}.\boldsymbol{m}^{-2}$	λ	9.4×10^{10}	$\mathbf{w}.\boldsymbol{m}^{-1}.\boldsymbol{k}^{-1}$	k_o	3860
$\mathbf{N}.\boldsymbol{m}^{-2}$	μ	4×10^{10}	$\boldsymbol{J}.\boldsymbol{m}^{-2}$	p	10^{10}
$\boldsymbol{kg}.\boldsymbol{m}^{-3}$	ρ	1740	$\boldsymbol{N}$	η	0.779×10^{-9}
K	θ_o	293	$\mathbf{N}.\boldsymbol{m}^{-2}.\boldsymbol{s}^{2}$	Π_1	0.1456×10^{-12}
Sec(s)	ϵ	0.02	$\mathbf{N}.\boldsymbol{m}^{-2}.\boldsymbol{s}^{2}$	Π_2	0.1546×10^{-12}
$\mathbf{N}.\boldsymbol{m}^{-2}$	K	10^{10}	N	ϑ_1	1.3×10^{-5}
$\mathbf{N}.\boldsymbol{m}^{-2}$	β_1^*	0.9×10^{10}	N	ϑ_2	0.12×10^{-5}
$\mathbf{N}.\boldsymbol{m}^{-2}$	β_2^*	0.1×10^{10}	N	ϑ_3	1.1×10^{-5}
$\mathbf{N}.\boldsymbol{m}^{-2}$	$\xi^*{}_1$	1.2×10^{6}	$\boldsymbol{K}^{-1}$	α_t	1.78×10^{-5}
$\mathbf{N}.\boldsymbol{m}^{-2}$	$\xi^*{}_2$	1.23×10^{6}	$\boldsymbol{m}^{2}$	ϖ	0.2×10^{-19}
$\mathbf{N}.\boldsymbol{m}^{-2}$	$\xi^*{}_3$	2.21×10^{10}	Sec(s)	t	0.5
$\mathbf{N}.\boldsymbol{m}^{-2}.\boldsymbol{k}^{-1}$	v_1	0.16×10^{5}	$\boldsymbol{m}$	L_N	7×10^{-6}
$\mathbf{N}.\boldsymbol{m}^{-2}.\boldsymbol{k}^{-1}$	v_2	0.219×10^{5}	$\boldsymbol{J}.\boldsymbol{Kg}^{-1}.\boldsymbol{K}^{-1}$	C_e	383.1

Table1: Numerical values of the material constants.

Figure 2 shows the variation of temperature θ, displacement u, normal stress σ_{xx}, shear stress σ_{xz}, equilibrated stress σ_x, ς_x, μ_{xy} and microrotation vector φ_2 along the $x-$axis for different times (t=0.1, 0.3, 0.5 and 0.7). All physical quantities increase with time, reflecting the progressive accumulation and diffusion of thermal energy in the medium. The temperature peaks at a specific location before decaying toward zero, demonstrating the interplay of thermal conduction and diffusion. Displacement grows over time due to thermal expansion driven by these gradients. Oscillatory stress patterns reveal the dynamic coupling of thermal and mechanical fields, while equilibrated stresses capture micropolar and nonlocal effects, including rotational microstructural contributions. These results highlight the time-dependent evolution of thermoelastic responses, emphasizing the need to consider transient thermal-mechanical interactions for accurate prediction of material behavior, structural stability, and thermal reliability. Overall, the θ, u, σ_{xx}, σ_{xz}, σ_x, ς_x, μ_{xy} and φ_2 increase with time t, indicating and it converges to zero with axial x increases . The values of t primarily influence the θ, u, σ_{xx}, σ_{xz},

σ_x, ς_x, μ_{xy} and $\varphi_2$magnitude, with higher values of either parameter leading to a θ, u, σ_{xx}, σ_{xz}, σ_x, ς_x, μ_{xy} and φ_2, followed by decay as distance increases. This result is in a good agreement with the results obtained by Abouelregal et al. [22].

Figure 3 reveals the variation of temperature θ, displacement u, normal stress σ_{xx}, shear stress σ_{xz}, equilibrated stress σ_x, ς_x, μ_{xy} and microrotation vector φ_2 with respect to x −axis for different values of rotation Ω namely (0, 0.3, 0.6 and 0.9) with thermal load. It is noticed that the magnitude of θ, u, σ_{xx}, σ_{xz} and ς_x is increasing with increasing Ω in the interval $0 \leq x \leq 10$. In contrast, the equilibrated stresses (σ_x, μ_{xy}, and φ_2) exhibit a decreasing trend as Ω increases within the same spatial domain. Across all rotation values, the temperature profile rises to a peak and then gradually declines, ultimately approaching zero as the distance increases. This convergence of temperature trends at larger *x*-values indicates diminishing thermal effects with distance from the heat source. The results provide deeper insight into the coupled thermo-mechanical behavior of the material system, highlighting how rotation significantly influences stress redistribution, and deformation patterns. In particular, rotation intensifies conventional stress and displacement responses while attenuating the equilibrated stress components. This interplay suggests that rotational effects play a dual role: enhancing mechanical responses while modulating nonlocal stress behaviors. Physically, the enhancement of displacement and stress arises from Coriolis and centrifugal forces, which amplify deformation and redistribute stresses. The reduction in equilibrated stresses reflects the modulation of microstructural stress contributions due to rotation, consistent with micropolar and nonlocal effects. These results demonstrate the dual role of rotation: intensifying classical thermoelastic responses while moderating microstructural stresses. This highlights the importance of accounting for rotational effects in predicting wave propagation, stress distribution, and deformation in rotating thermoelastic media. The θ, u, σ_{xx}, σ_{xz}, σ_x, ς_x, μ_{xy} and φ_2 exhibit a characteristic rise and it converges to zero with axial x increases. This result is in a good agreement with the results obtained by Kumar and Vohra [18]

Figure 4 shows the variation of temperature θ, displacement u, normal stress σ_{xx}, shear stress σ_{xz}, equilibrated stress σ_x, ς_x, μ_{xy} and microrotation vector φ_2 along the x −axis for different values of the initial stress p (p = 0, 5× 10^{10}, 7 × 10^{10}, and 9 × 10^{10}) under thermal loading. Within the region $0 \leq x \leq 10$, the magnitudes of θ, u, and ς_x increase with

increasing initial stress, indicating that pre-stress enhances the thermoelastic coupling and intensifies the thermal and mechanical responses of the medium.

Physically, the presence of initial stress alters the effective stiffness of the material and modifies the stress–strain relationship, leading to amplified deformation and higher stress levels when the medium is subjected to thermal excitation. The temperature profiles exhibit a rise to a peak followed by a gradual decay toward zero as the distance increases, reflecting the finite-speed heat propagation and the attenuation of thermal waves predicted by the Moore–Gibson–Thompson theory.

In contrast, the quantities σ_{xx}, σ_{xz}, σ_x, μ_{xy} and φ_2 decrease with increasing initial stress. This behavior can be attributed to the redistribution of internal forces caused by pre-stress, which suppresses shear deformation and weakens the contribution of nonlocal and microstructural stress interactions. Moreover, the microrotation field φ_2 is noticeably affected by the initial stress, confirming the sensitivity of micropolar effects to the pre-existing mechanical state of the medium. Overall, the results demonstrate that initial stress plays a dual role in the system response: it amplifies the classical thermoelastic fields such as temperature, displacement, and normal stress, while simultaneously attenuating certain equilibrated and microstructural stress components. This highlights the complex interaction between initial stress, thermal loading, rotation, and nonlocal micropolar effects in governing wave propagation and stress redistribution in double-porous thermoelastic media. The θ, u, σ_{xx}, σ_{xz}, σ_x, ς_x, μ_{xy} and φ_2 reveals how uncertainties in thermal and mechanical excitation influence wave propagation, which is particularly important in high-precision applications. This result is in a good agreement with the results obtained by Gupta et al. [15].

Figure 5 illustrates how temperature θ, displacement u, normal stress σ_{xx}, shear stress σ_{xz}, equilibrated stress σ_x, ς_x, μ_{xy} and microrotation vector φ_2 vary along the x-direction for several values of the nonlocal parameter (L_n = 0, 1×10^{-5}, 1.3×10^{-5}, and 1.6×10^{-5}) under thermal loading. Within the range$0 \le x \le 10$, an increase in L_n leads to higher values of temperature, displacement, shear stress, and ς_x. On the other hand, the normal stress, equilibrated stress components, and microrotation decrease as the nonlocal effect becomes stronger over the same spatial interval. This contrasting behavior highlights the influence of nonlocal interactions in enhancing global thermal and deformation responses while simultaneously reducing localized stress and microstructural effects. This behavior reflects the stress-smoothing effect of nonlocal elasticity, which reduces localized stress

concentrations and weakens microstructural and micro rotational responses. Overall, the results demonstrate that nonlocality amplifies global thermal and displacement fields while attenuating localized stress and microrotation effects in the thermoelastic medium. This result is in a good agreement with the results obtained by Gupta et al. [13].

6. Conclusion and Limitations

This study presented a comprehensive analytical model for a two-dimensional rotating, nonlocal micropolar double-porous thermoelastic medium under Moore–Gibson–Thompson (MGT) theory. Using normal mode analysis, exact solutions were derived for displacement, microrotation, temperature, and stress fields. Numerical illustrations were performed to assess the effects of time, rotation, initial stress, and nonlocal parameters. The key findings are summarized as follows:

- All physical variables temperature, displacement, and stresses grow over time, indicating progressive thermal and mechanical responses under applied loads.
- Rotation and initial stress significantly amplify the magnitude of thermal and mechanical responses, altering wave amplitudes and arrival times.
- Incorporating the nonlocal parameter enhances size-dependent behavior, affecting stress and displacement distributions, particularly near the surface.
- Temperature exhibits combined wave-like and diffusive behavior, while displacement fields show elastic wave fronts modulated by thermal effects.
- The distribution and magnitude of stresses and displacements are strongly influenced by boundary constraints and loading conditions, confirming the model's consistency.
- The presence of macro- and micro-pores affects the amplitude and phase of thermal and elastic waves, highlighting the role of microstructure.
- Results provide insights for applications in geophysics, seismology, earthquake engineering, and material design, particularly in systems involving rotation, double porosity, and nonlocal interactions.
- The results are directly applicable to rotating porous microstructured materials in geothermal, laser-heating, and microscale engineering applications, where nonlocal and memory-dependent thermoelastic effects cannot be neglected.

The study demonstrates the importance of accounting for rotation, initial stress, nonlocal effects, and double porosity in predicting realistic thermoelastic responses, providing a solid framework for future theoretical and applied investigations.

The present analysis is developed within the framework of linear generalized thermoelasticity, assuming isotropic material behavior and small deformations. These assumptions ensure mathematical tractability and are appropriate for moderate thermal loads and elastic responses; however, they may limit applicability under large strains or strong nonlinear effects. The solution is obtained using normal mode analysis, which is well suited for studying wave propagation in semi-infinite media but restricts the investigation to harmonic disturbances and idealized boundary conditions. Consequently, complex transient or localized loading scenarios are not fully captured. Furthermore, the model is formulated in a one-dimensional setting. Extending the present approach to three-dimensional configurations or nonlinear regimes would introduce significant mathematical and computational challenges and is left for future investigations.

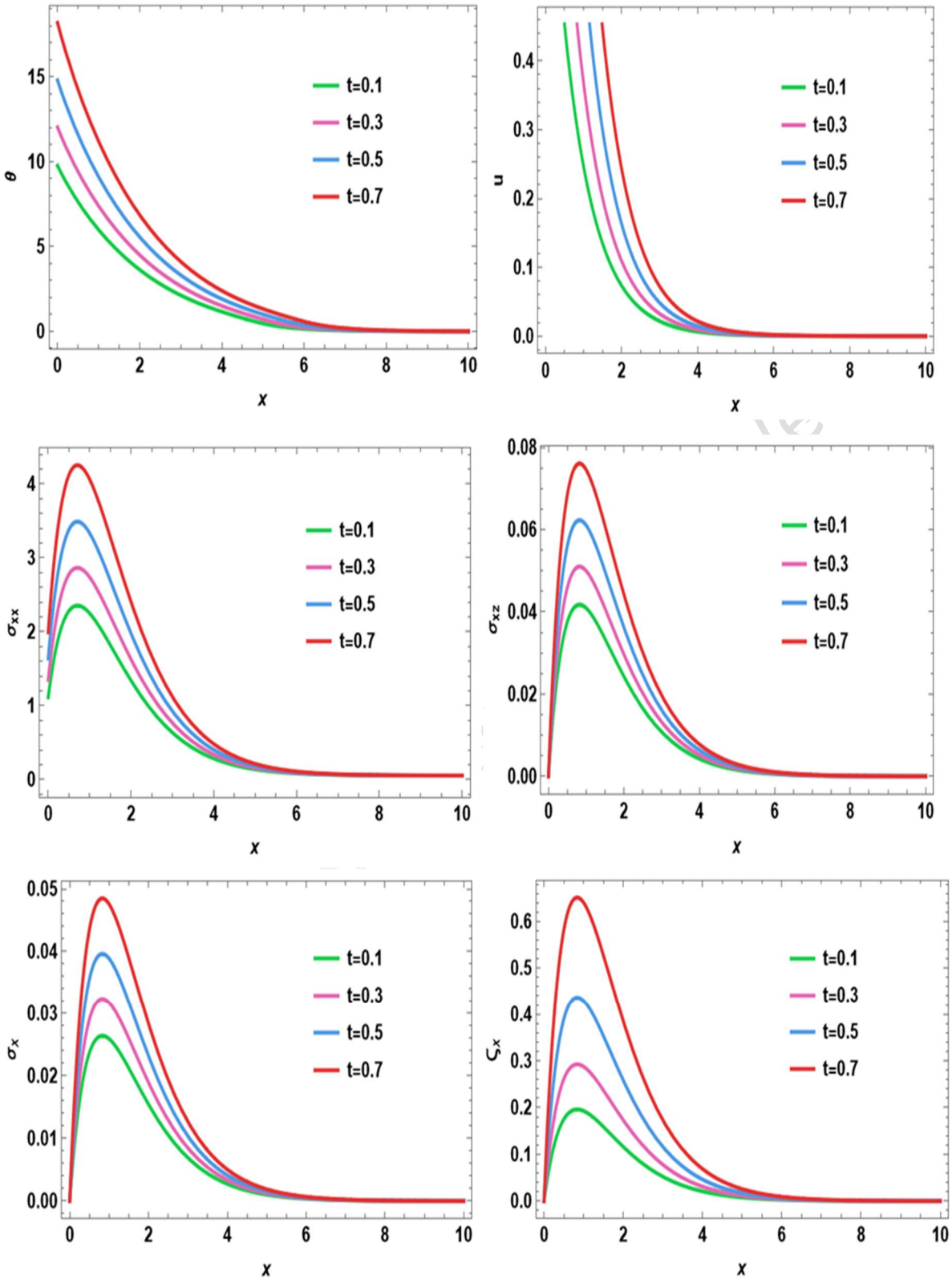

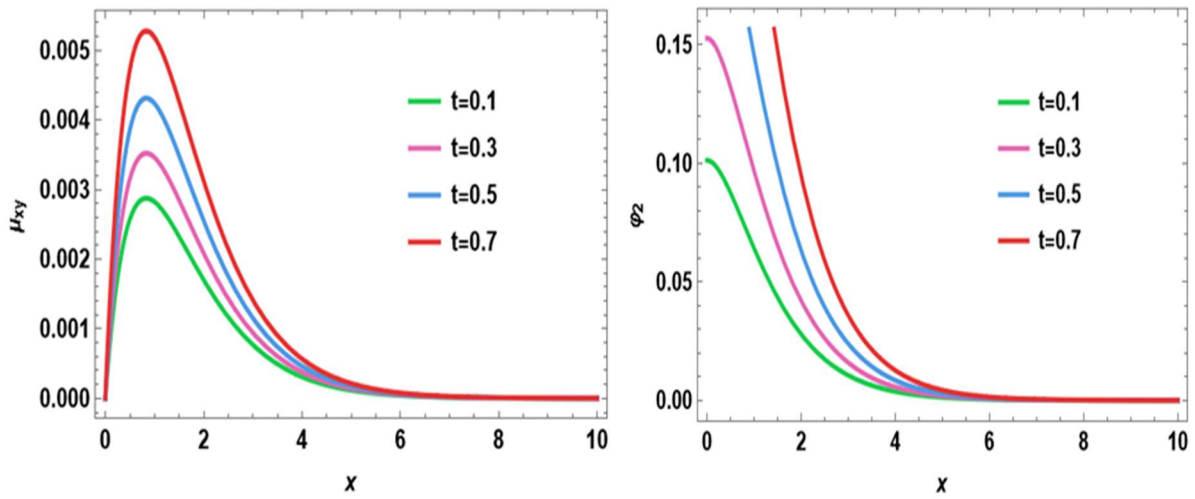

Figure 2: The influence of time on all physical quantities with distance *x*.

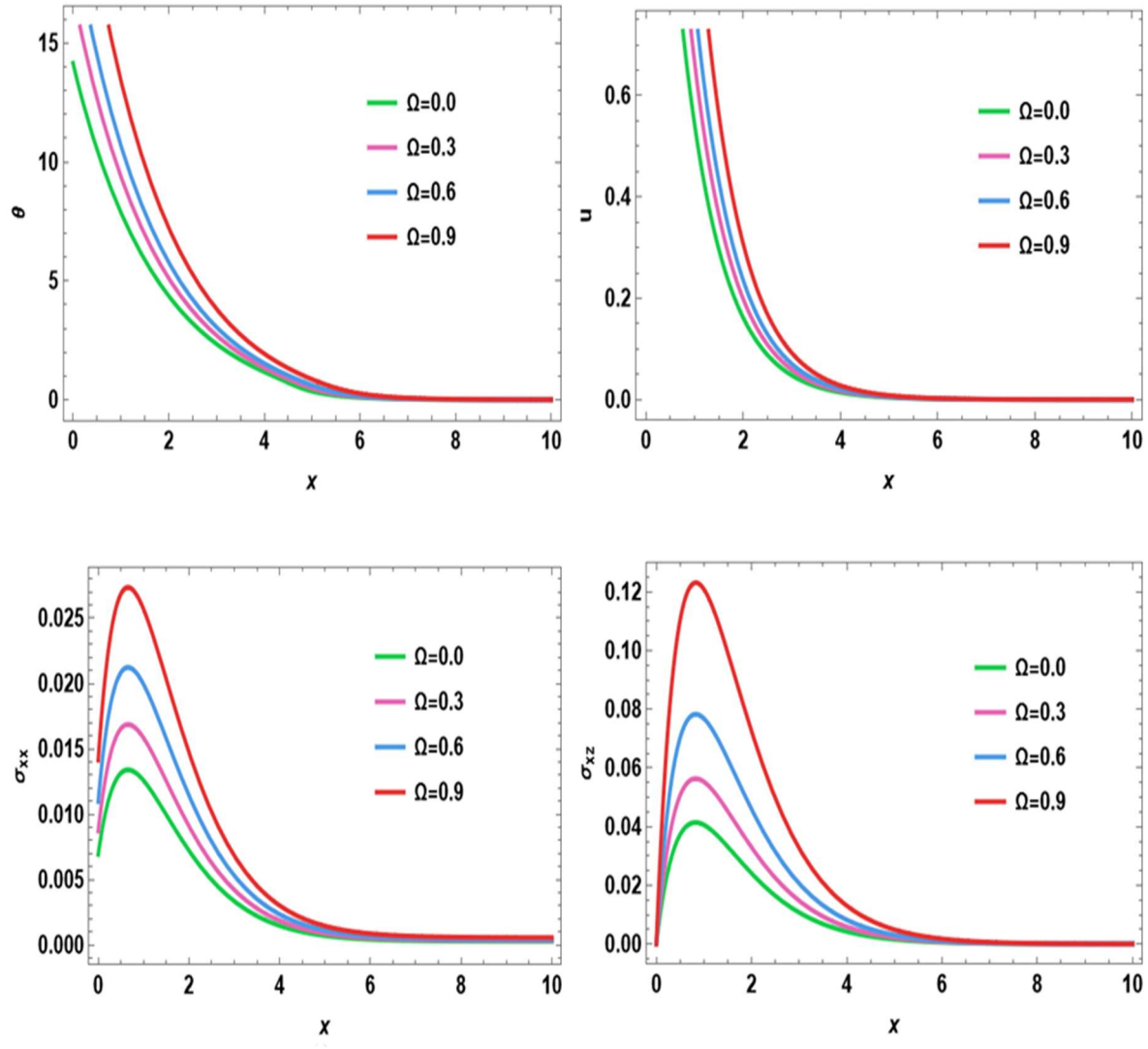

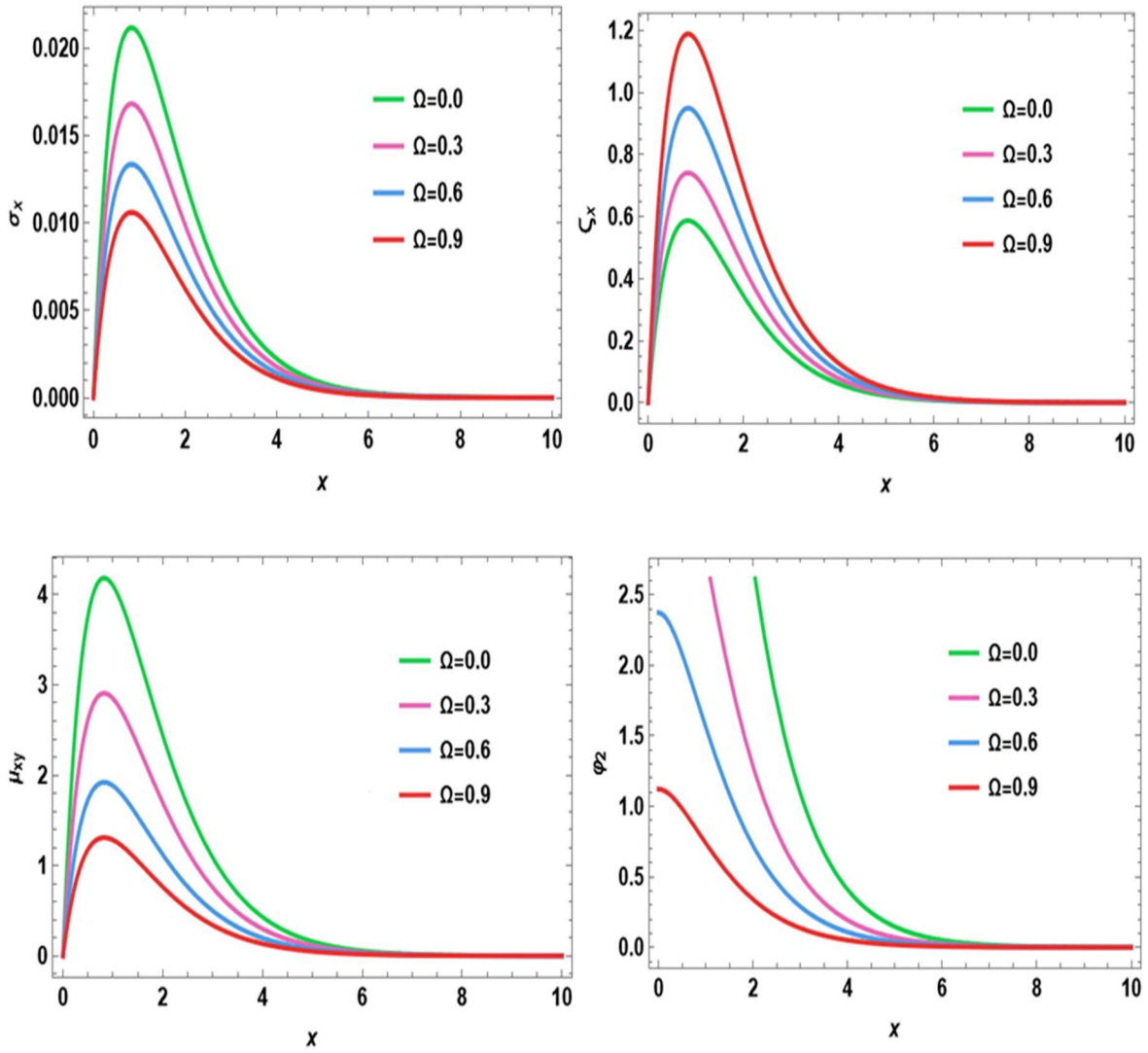

Figure 3: The influence of rotation on all physical quantities with distance x.

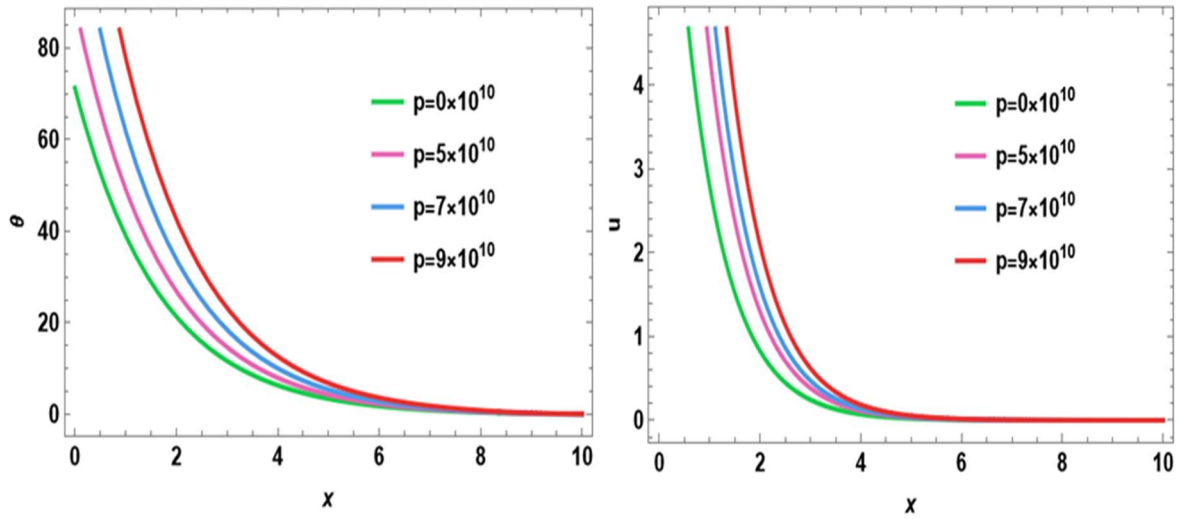

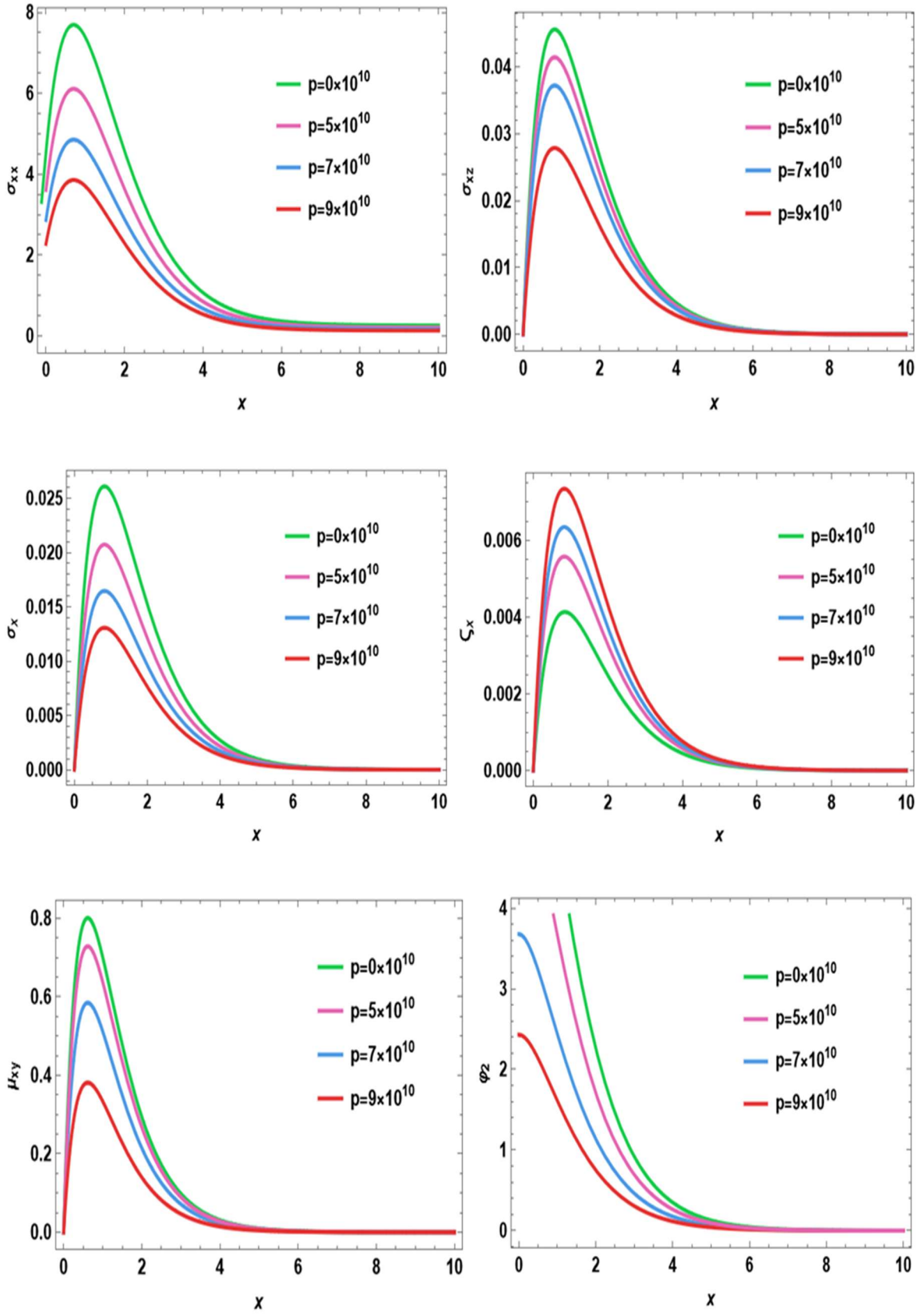

Figure 4: The influence of initial stress on all physical quantities with distance *x*.

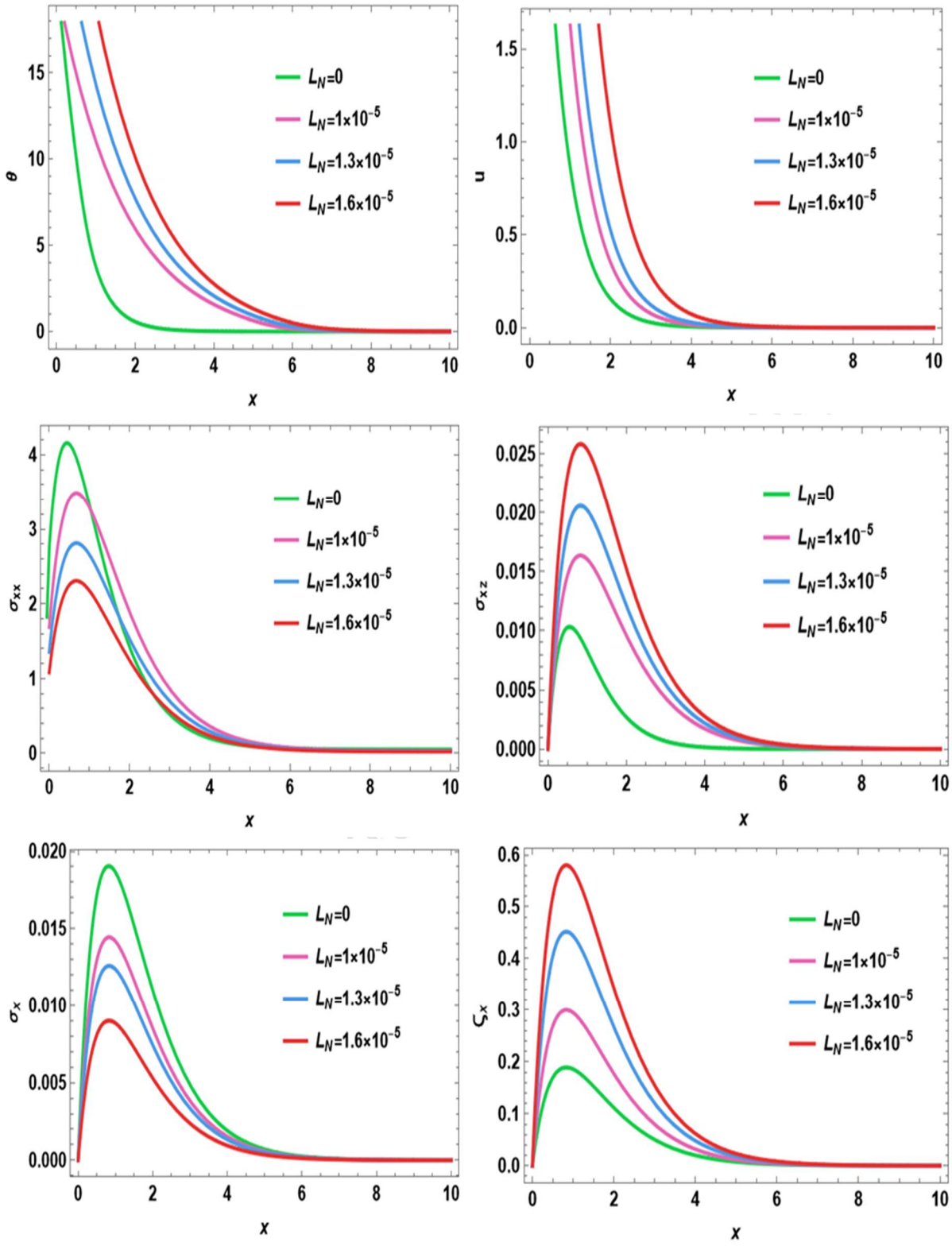

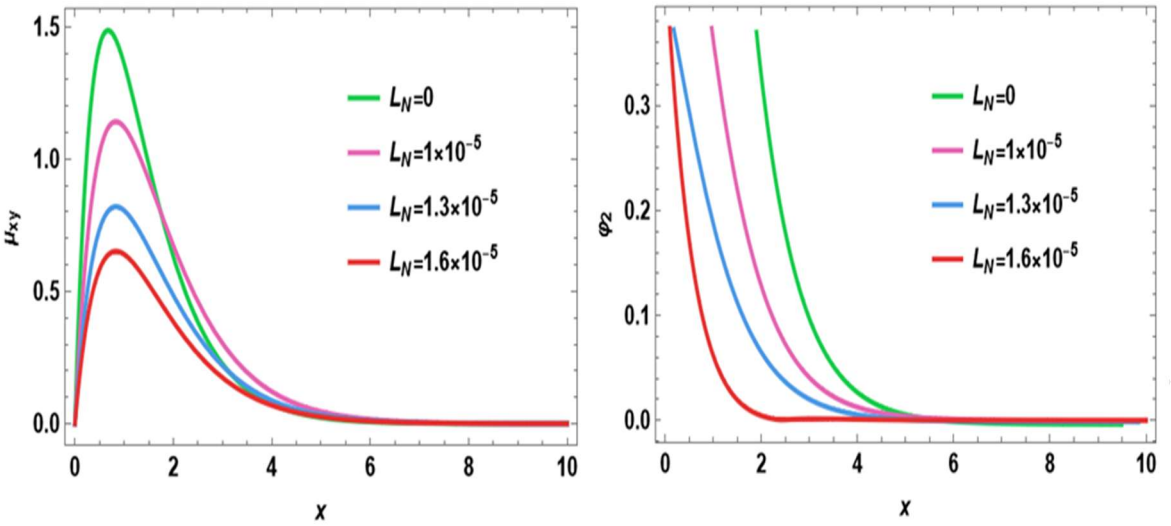

Figure 5: The influence of nonlocal on all physical quantities with distance *x*.

Funding: This work was supported by the Deanships of Scientific Research, Vice Presidency for Graduate Studies and Scientific Research, King Faisal University, Saudi Arabia (Grant No. KFU253964)

References:

[1] M.A. Biot, Thermoelasticity and irreversible thermodynamics, Journal of Applied Physics, 27(3), 240–253, (1956). https://doi.org/10.1063/1.1722351.

[2] H.W. Lord, Y. Shulman, A generalized dynamical theory of thermoelasticity, Journal of the Mechanics and Physics of Solids, 15(5), 299–309, (1967). https://doi.org/10.1016/0022-5096(67)90024-5.

[3] A.E. Green, K.A. Lindsay, Thermoelasticity, Journal of Elasticity, 2, 1–7, (1972). https://doi.org/10.1007/BF00045689.

[4] A.E. Green, P.M. Naghdi, Thermoelasticity without energy dissipation, Journal of Elasticity, 31, 189–208, (1993). https://doi.org/10.1007/BF00044969.

[5] D. M. Salah, and A. M. Abd-Alla, Effect of initial stress and rotation on magneto-thermoelastic half-space with gravity field and without energy dissipation**,** The Journal of Strain Analysis for Engineering Design, 59 (1), (2023). https://doi.org/10.1177/03093247231188762.

[6] K. Boora, A. Kadian, and S. Deswal, Reflection of plane waves in an initially stressed thermodiffusion medium under double porosity effect, Journal of Vibration Engineering Technologies, 12, 879–5892, (2024). https://doi.org/10.1007/s42417-023-01225-8.

[7] M. I. A. Othman, R. S. Tantawi, and E. M. Abd-Elaziz, Effect of initial stress on a thermoelastic medium with voids and microtemperatures, Journal of Porous Media, 19(2), 155–172, (2016). 10.1615/JPorMedia.v19.i2.40.

[8] A.C. Eringen, Theory of nonlocal thermoelasticity, International Journal of Engineering Science, 12, 1063–1077, (1974). https://doi.org/10.1016/0020-7225(74)90033-0.

[9] D. Iesan, and R. Quintanilla, On the theory of thermoelastic materials with a double porosity structure, Journal of Thermal Stresses, 37(9), 1017–1036, (2014). Doi: 10.1080/01495739.2014.914776.

[10] A. M. Zenkour, A. E. Abouelregal AE, K. A. Alnefaie, X. Zhang and E. C. Aifantis, Nonlocal thermoelasticity theory for thermal-shock nanobeams with temperature-dependent thermal conductivity, Journal of Thermal Stresses, 38(9), 1049–1067, (2015). https://doi.org/10.1080/01495739.2015.1038490.

[11] P. Luo, X. Li and X. Tian, Nonlocal thermoelasticity and its application in thermoelastic problem with temperature-dependent thermal conductivity, European Journal of Mechanics / A Solids, 87, 104204, (2021). doi.org/10.1016/j.euromechsol.2020.104204.

[12] D. M. Salah, A. M. Abd-Alla, S. M. Abo-Dahab, A. M. Alharbi and M. A. Abdelhafez, Magneto-Thermoelastic Semiconductor Medium with Diffusion under the Hyperbolic Two-Temperature Photothermal Waves, Mechanics of Solids, 59, 1774–1791, (2024). https://doi.org/10.1134/S0025654424603768.

[13] S. Gupta, R. Dutta and S. Das, Memory response in a nonlocal micropolar double porous thermoelastic medium with variable conductivity under Moore-Gibson-Thompson thermoelasticity theory, Journal of Ocean Engineering and Science, 8, 263–277, (2023). https://doi.org/10.1016/j.joes.2022.01.010.

[14] E. Awwad, Ahmed E. Abouelregal, A. Soleiman, Thermoelastic Memory-dependent Responses to an Infinite Medium with a Cylindrical Hole and Temperature-dependent Properties, Journal of Applied and Computational Mechanics, 7(2), 870-882, (2021). Doi: 10.22055/jacm.2021.36048.2784.

[15] S. Gupta, S. Das, R. Dutta and A. K. Verma, Higher-order fractional and memory response in nonlocal double poro-magneto-thermoelastic medium with temperature-dependent properties excited by laser pulse, Journal of Ocean Engineering and Science, (2022). https://doi.org/10.1016/j.joes.2022.04.013.

[16] R. Kumar, N. Sharma and S. Chopra, Photothermoelastic interactions under Moore-GibsonThompson thermoelasticity, Journal of Coupled Systems Mechanics, 11(5), 459-483, (2022). https://doi.org/10.12989/csm.2022.11.5.459.

[17] R. Tiwari, A. M. Saeed, R. Kumar, A. Kumar, and A. Singhal, Memory response on generalized thermoelastic medium in context of dual phase lag thermoelasticity with non-local effect, Journal of Archives of Mechanics, 74 (2-3), 69–88, (2022).

Doi: 10.24423/aom.3926.

[18] R. Kumar and R. Vohra, Response of thermoelastic microbeam with double porosity structure due to pulsed laser heating, Journal of Mechanics and Mechanical Engineering, 23, 76–85, (2019). **Doi:**10.2478/mme-2019-0011.

[19] A. E. Abouelregal, I. Dassios, and O. Moaaz, Moore–Gibson–Thompson thermoelastic model effect of laser-induced microstructures of a microbeam sitting on visco-pasternak foundations, Journal of applied sciences, 12, 9206, (2022).

https://doi.org/10.3390/app12189206.

[20] Y. Alhassan, M. Alsubhi and A. E. Abouelregal, A modified Moore-Gibson-Thompson fractional model for mass diffusion and thermal behavior in an infinite elastic medium with a cylindrical cavity, Journal of Aims Mathematics, 9 (8), 21860–21889, (2024). doi: 10.3934/math.20241063.

[21] M. Marin and O. Florea, On temporal behaviour of solutions in thermoelasticity of porous micropolar bodies, An. St. Univ. Ovidius Constanta 22(1), 169-188 (2014). DOI: 10.2478/auom-2014-0014.

[22] A. E. Abouelregal, M. Marin and A. Öchsner, The influence of a non-local Moore–Gibson–Thompson heat transfer model on an underlying thermoelastic material under the model of memory-dependent derivatives, Continuum Mechanics and Thermodynamics, 35, 545–562, (2023). https://doi.org/10.1007/s00161-023-01195-y.

[23] A. Zeeshan, M. Imran Khan, R. Ellahi and M. Marin, Computational Intelligence Approach for Optimising MHD Casson Ternary Hybrid Nanofluid over the Shrinking Sheet with the Effects of Radiation, Applied Sciences, 13(17), (2023).

https://doi.org/10.3390/app13179510.

[24] R. M. Kumar, R. S. Raju, F. Mebarek-Oudina, M. A. Kumar and V. K. Narla, Cross-Diffusion Effects on an MHD Williamson Nanofluid Flow Past a Nonlinear Stretching Sheet Immersed in a Permeable Medium, Frontiers in Heat and Mass Transfer, 22(1), 15-34, (2024). https://doi.org/10.32604/fhmt.2024.048045.

[25] T. Naseem, F. Mebarek-Oudina, H. Vaidya, N. Bibi, K. Ramesh, S. U. Khan, Numerical Analysis of Entropy Generation in Joule Heated Radiative Viscous Fluid Flow over a Permeable Radially Stretching Disk, CMES - Computer Modeling in Engineering and Sciences, 134(1), 351-371, (2025). https://doi.org/10.32604/cmes.2025.063196.

[26] H. Vaidya, F. Mebarek-Oudina, K. V. Prasad, R. Choudhari, N.Z. Basha, S. Kalal, Nanofluid Flow across a Moving Plate under Blasius-Rayleigh-Stokes (BRS) Variable Transport Fluid Characteristics, Frontiers in Heat and Mass Transfer, 22(1), 65-78, (2024). https://doi.org/10.32604/fhmt.2024.047879.

[27] M. A. Kumar, F. Mebarek-Oudina, P. Mangathai, N. A. Shah, Ch. Vijayabhaskar, N. Venkatesh, and Y. Fouad, The impact of Soret Dufour and radiation on the laminar flow of a rotating liquid past a porous plate via chemical reaction, Modern Physics Letters B, 39(10), 2450458, (2025). https://doi.org/10.1142/S021798492450458X.

[28] F. Mebarek-Oudina, M. Bouselsal, R. Djebali, H. Vaidya, N. Biswas, and K. Ramesh, Thermal performance of MgO-SWCNT/water hybrid nanofluids in a zigzag walled cavity with differently shaped obstacles, Modern Physics Letters B, 39 (29), 2550163, (2025). https://doi.org/10.1142/S0217984925501635.

[29] F. M. Oudina, G. Dharmaiah, J.L.R. Prasad, H. Vaidya, M.A. Kumari, Thermal and Flow Dynamics of Magnetohydrodynamic Burgers' Fluid Induced by a Stretching Cylinder

with Internal Heat Generation and Absorption, International Journal of Thermofluids, 25, 100986, (2025). https://doi.org/10.1016/j.ijft.2024.100986.

[30] Doaa. M. Salah, A.M. Abd-Alla, SMM El-Kabeir, Influence of nonlocal on a rotating thermoelastic medium with diffusion and double porosity, Scientific Reports, 15, 15955, (2025). https://doi.org/10.1038/s41598-025-97334-3.

[31] Doaa. M. Salah, A.M. Abd-Alla, SMM El-Kabeir, Magneto-Thermoelastic Response of a Rotating Medium with Double Porosity under Initial Stress, Mechanics of Solids, (2025). https://doi.org/10.1134/S0025654425602010.

Appendix A

$\xi = r_{16}r_{21}r_{29}r_{33} - r_{29}r_{33}r_{41}r_{46}$,

$A_{11} = \frac{1}{\xi}(-r_{16}r_{21}r_{29}r_{32} + r_6r_{16}r_{20}r_{33} + r_7r_{21}r_{33} - r_{16}r_{21}r_{28}r_{33} - r_5r_{16}r_{21}r_{34} - r_7r_{20}r_{33}r_{41} - r_{21}r_{29}r_{33}r_{43} - r_{16}r_{29}r_{33}r_{45} - r_6r_{33}r_{46} + r_{29}r_{32}r_{41}r_{46} + r_{28}r_{33}r_{41}r_{46} + r_5r_{34}r_{41}r_{46} + r_{29}r_{33}r_{42}r_{46} + r_{29}r_{33}r_{41}r_{47})$,

$A_{22} = \frac{1}{\xi}(-r_6r_{16}r_{20}r_{32} - r_7r_{21}r_{32} + r_{16}r_{21}r_{28}r_{32} - b^2r_7r_{21}r_{33} - r_7r_{19}r_{21}r_{34} - r_6r_{16}r_{25}r_{34} + r_5r_{16}r_{21}r_{35} - r_5r_{16}r_{20}r_{36} + r_{16}r_{25}r_{29}r_{36} - r_5r_{21}r_{37} + r_{19}r_{21}r_{29}r_{37} + r_7r_{20}r_{32}r_{41} + r_7r_{25}r_{34}r_{41} + r_5r_{20}r_{37}r_{41} - r_{25}r_{29}r_{37}r_{41} + r_7r_{20}r_{33}r_{42} + r_{21}r_{29}r_{32}r_{43} - r_6r_{20}r_{33}r_{43} + r_{21}r_{28}r_{33}r_{43} + r_5r_{21}r_{34}r_{43} - r_6r_{16}r_{33}r_{44} + r_7r_{33}r_{41}r_{44} + r_{16}r_{29}r_{32}r_{45} - r_7r_{33}r_{45} + r_{16}r_{28}r_{33}r_{45} + r_5r_{16}r_{34}r_{45} + r_{29}r_{33}r_{43}r_{45} + r_6r_{32}r_{46} + b^2r_6r_{33}r_{46} + r_6r_{19}r_{34}r_{46} + r_5r_{36}r_{46} - r_{19}r_{29}r_{36}r_{46} - r_{28}r_{32}r_{41}r_{46} - r_5r_{35}r_{41}r_{46} - r_{29}r_{32}r_{42}r_{46} - r_{28}r_{33}r_{42}r_{46} - r_5r_{34}r_{42}r_{46} + r_6r_{33}r_{47} - r_{29}r_{32}r_{41}r_{47} - r_{28}r_{33}r_{41}r_{47} - r_5r_{34}r_{41}r_{47} - r_{29}r_{33}r_{42}r_{47})$,

$A_{33} = \frac{1}{\xi}(b^2r_7r_{21}r_{32} + r_7r_{19}r_{21}r_{35} + r_6r_{16}r_{25}r_{35} - r_7r_{19}r_{20}r_{36} + r_7r_{25}r_{36} - r_{16}r_{25}r_{28}r_{36} + r_6r_{19}r_{20}r_{37} + b^2r_5r_{21}r_{37} - r_6r_{25}r_{37} - r_{19}r_{21}r_{28}r_{37} - r_7r_{25}r_{35}r_{41} + r_{25}r_{28}r_{37}r_{41} - r_7r_{20}r_{32}r_{42} - r_7r_{25}r_{34}r_{42} - r_5r_{20}r_{37}r_{42} + r_{25}r_{29}r_{37}r_{42} + r_6r_{20}r_{32}r_{43} - r_{21}r_{28}r_{32}r_{43} + r_6r_{25}r_{34}r_{43} - r_5r_{21}r_{35}r_{43} + r_5r_{20}r_{36}r_{43} - r_{25}r_{29}r_{36}r_{43} + r_6r_{16}r_{32}r_{44} + r_5r_{16}r_{36}r_{44} - r_7r_{32}r_{41}r_{44} - r_5r_{37}r_{41}r_{44} - r_7r_{33}r_{42}r_{44} + r_6r_{33}r_{43}r_{44} + r_7r_{32}r_{45} - r_{16}r_{28}r_{32}r_{45} + b^2r_7r_{33}r_{45} + r_7r_{19}r_{34}r_{45} - r_5r_{16}r_{35}r_{45} + r_5r_{37}r_{45} - r_{19}r_{29}r_{37}r_{45} - r_{29}r_{32}r_{43}r_{45} - r_{28}r_{33}r_{43}r_{45} - r_5r_{34}r_{43}r_{45} - b^2r_6r_{32}r_{46} - r_6r_{19}r_{35}r_{46} - b^2r_5r_{36}r_{46} + r_{19}r_{28}r_{36}r_{46} +$

$r_{28}r_{32}r_{42}r_{46} + r_5r_{35}r_{42}r_{46} - r_6r_{32}r_{47} - b^2r_6r_{33}r_{47} - r_6r_{19}r_{34}r_{47} - r_5r_{36}r_{47} + r_{19}r_{29}r_{36}r_{47} + r_{28}r_{32}r_{41}r_{47} + r_5r_{35}r_{41}r_{47} + r_{29}r_{32}r_{42}r_{47} + r_{28}r_{33}r_{42}r_{47} + r_5r_{34}r_{42}r_{47})$,

$A_{44} = \frac{1}{\xi}(-b^2r_7r_{25}r_{36} + b^2r_6r_{25}r_{37} + r_7r_{25}r_{35}r_{42} - r_{25}r_{28}r_{37}r_{42} - r_6r_{25}r_{35}r_{43} + r_{25}r_{28}r_{36}r_{43} + r_7r_{19}r_{36}r_{44} - r_6r_{19}r_{37}r_{44} + r_7r_{32}r_{42}r_{44} + r_5r_{37}r_{42}r_{44} - r_6r_{32}r_{43}r_{44} - r_5r_{36}r_{43}r_{44} - b^2r_7r_{32}r_{45} - r_7r_{19}r_{35}r_{45} - b^2r_5r_{37}r_{45} + r_{19}r_{28}r_{37}r_{45} + r_{28}r_{32}r_{43}r_{45} + r_5r_{35}r_{43}r_{45} + b^2r_6r_{32}r_{47} + r_6r_{19}r_{35}r_{47} + b^2r_5r_{36}r_{47} - r_{19}r_{28}r_{36}r_{47} - r_{28}r_{32}r_{42}r_{47} - r_5r_{35}r_{42}r_{47})$,

$B_{11} = \frac{-r_{31}r_{38}-r_{30}r_{39}+r_4r_{13}}{r_{31}r_{39}}$, $B_{22} = \frac{r_{30}r_{38}-r_4r_{40}}{r_{31}r_{39}}$.